12-2002

Online Determination of the Steady-State Condition of an Aerodynamic Test Article Mounted in a Wind Tunnel Test Cell

Martin Vincent Fette

University of Tennessee - Knoxville

To the Graduate Council:

I am submitting herewith a thesis written by Martin Vincent Fette entitled "Online Determination of the Steady-State Condition of an Aerodynamic Test Article Mounted in a Wind Tunnel Test Cell." I have examined the final electronic copy of this thesis for form and content and recommend that it be accepted in partial fulfillment of the requirements for the degree of Master of Science, with a major in Electrical Engineering.

Bruce W. Bomar, Major Professor

We have read this thesis and recommend its acceptance:

Roy D. Joseph, L. Montgomery Smith

Accepted for the Council:
Carolyn R. Hodges

Vice Provost and Dean of the Graduate School

(Original signatures are on file with official student records.)

To the Graduate Council:

I am submitting herewith a thesis written by Martin Vincent Fette entitled "Online Determination of the Steady-State Condition of an Aerodynamic Test Article Mounted in a Wind Tunnel Test Cell." I have examined the final electronic copy of this thesis for form and content and recommend that it be accepted in partial fulfillment of the requirements for the degree of Master of Science, with a major in Electrical Engineering.

Bruce W. Bomar
Major Professor

We have read this thesis and
recommend its acceptance:

Roy D. Joseph

L. Montgomery Smith

Acceptance for the Council:

Anne Mayhew
Vice Provost and Dean of Graduate Studies

(Original signatures are on file with official student records.)

ONLINE DETERMINATION OF THE STEADY-STATE CONDITION OF AN AERODYNAMIC TEST ARTICLE MOUNTED IN A WIND TUNNEL TEST CELL

A Thesis
Presented for the
Master of Science
Degree
The University of Tennessee, Knoxville

Martin Vincent Fette
December 2002

ACKNOWLEDGEMENTS

The author wishes to thank Dr. Bruce Bomar, Dr. Roy Joseph, and Dr. L. Montgomery Smith for their advice and assistance in the preparation of this thesis. Appreciation is also expressed to the University of Tennessee Space Institute, the United States Air Force (USAF), the Arnold Engineering Development Center (AEDC), and the management of Sverdrup Technology, Inc., AEDC Group, for the opportunity to pursue this graduate degree and the resources required to complete this masters thesis.

The author also wishes to thank Mr. Steve Carter, Mr. Rob Mathis and Dr. Bill Lawrence for their advice and assistance throughout this study.

The research reported herein was performed by the AEDC, Air Force Materiel Command. Work and analysis for this research was completed by personnel of Sverdrup Technology, Inc., AEDC Group, support contractor for the AEDC propulsion test facilities. Approved for Public Release; Distribution is unlimited. Further reproduction is authorized to satisfy the needs of the U.S. Government.

ABSTRACT

The Propulsion Wind Tunnel (PWT) facility at Arnold Engineering Development Center is devoted to aerodynamic and propulsion integration testing of large-scale aerodynamic models. Models of aircraft, missiles and rockets are tested at simulated altitude conditions from sea level to about 150,000 feet.

Before the data acquisition sequence, it is necessary to establish that the model position has stabilized following the movement of the test model to a new orientation. The existing procedure requires an extra delay, after moving the model, before data is acquired. This delay, however, may be more or less than necessary, resulting in wasted testing time or compromised data quality. This wasted time can be attributed to excessive delays (i.e. the model was already stabilized) or the need to retake a point that was not adequately settled. In this thesis, an alternate approach is developed and evaluated for estimating in real time when the model position can be considered settled.

The research effort determined that a system of this type was both feasible and realizable. Since the raw model position data includes a wide spectrum of noise, two types of digital filters were evaluated. These were a finite impulse response (FIR) filter and an infinite impulse response (IIR) filter. Experimental results showed that the data system should apply an Infinite Impulse Response filter on data sampled independently from the main facility data acquisition system.

Once the test data was filtered, a separate algorithm was employed to make the steady state determination. Several algorithms were evaluated and verified against 60

data sets for accuracy and predictive qualities. The final choice compares the derivative of filtered position data with a predetermined threshold value. This approach returned the best results when compared to a visual inspection of the data.

TABLE OF CONTENTS

LIST OF FIGURES

FIGURE

LIST OF TABLES

TABLE

CHAPTER I
INTRODUCTION

Arnold Engineering Development Center houses one of the largest collections of flight simulation test facilities in the world. AEDC is a unit of the Air Force Material Command and is a test and evaluation center for the United States Air Force and the Department of Defense. Engineers at AEDC have been involved in the development of nearly all U.S. military high performance aircraft as well as many NASA space systems.

Testing at AEDC is divided into three major categories: Aerodynamics, Aeropropulsion, and Space and Missiles. Aerodynamic testing includes the measurement of performance, stability, control systems, and aerodynamic load of an aircraft or other aerodynamic model. Aeropropulsion testing concentrates on the aircraft propulsion system and on the performance characteristics of these engines under varied flight-test conditions. Finally, the Space and Missiles department evaluates the performance of entire rocket systems, from the engine to the flight controls. This department also includes resources for evaluating system performance in the vacuum and hard radiation environments of the type expected in space.

The majority of the aerodynamic testing is performed in AEDC's large wind tunnel group called the Propulsion Wind Tunnel facility. The facility has two sixteen foot wind tunnels - one supersonic (16S) and one transonic (16T). These tunnels are primarily utilized to measure the aerodynamic performance of large aircraft models or large-scale missiles. A four-foot wind tunnel (4T) is also utilized for aerodynamic

measurements - primarily aircraft store separation. Proper store separation from an aircraft ensures that fuel tanks, missiles, or other externally carried components fall clear of the aircraft during a jettison or launch.

The Propulsion Wind Tunnel (PWT) facilities are used for conventional aerodynamic tests and for combined aerodynamic/propulsion system tests. Large and full-scale models of aircraft, missiles and rockets are tested at simulated altitude conditions from sea level to about 150,000 feet. Scale replicas are mounted on calibrated sensors and the forces exerted on the model by the airstream are measured.

The measured aerodynamic properties include the drag, crosswind force, and lift; also the rolling, pitching, and yawing moments. In aerodynamic testing, conditioned air is blown past a stationary model and the stability, control systems, and aerodynamic flight characteristics are tested. A calibrated device, known as the six-component balance measures the forces exerted on the model in the air stream. The balance returns an analog voltage proportional to the force exerted on the aerodynamic model by the airstream. This signal is measured and conditioned with both analog and digital filters that are pre-determined by customer requirements and implemented prior to the test.

Figure 1 shows a subscale model of a Boeing 747 mounted in the 16T test chamber. These chambers are equipped with moveable supports, called stings, for mounting test articles. To simulate change in flight attitude or maneuvers, the support is rolled or pitched up or down while simulated flight conditions are maintained.

Figure 1 -Picture of a model installed in the PWT

– photo courtesy of AEDC Public Affairs Department

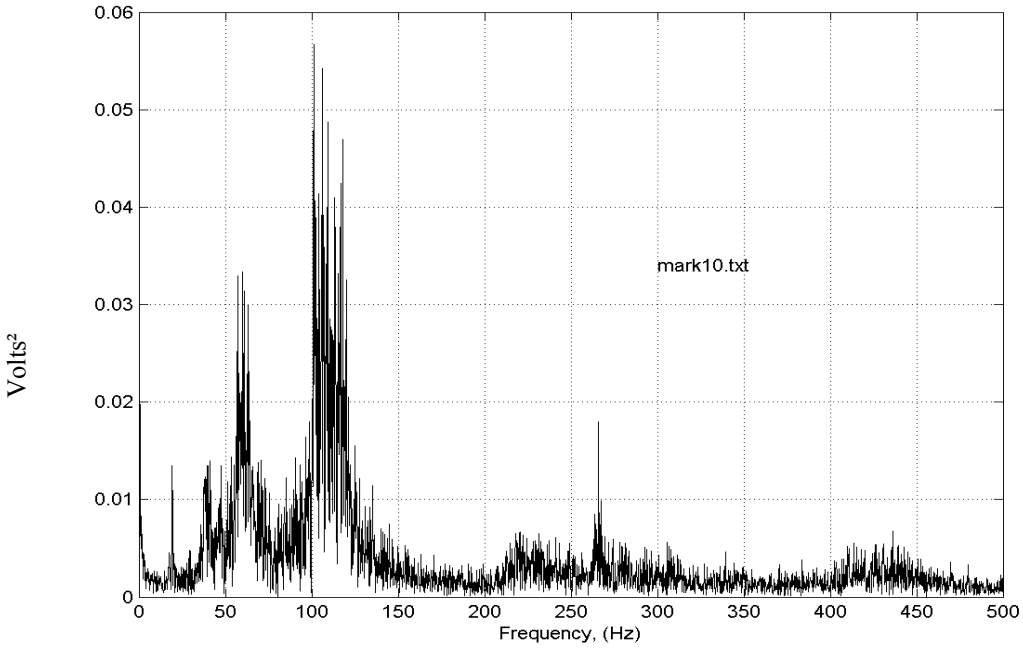

Figure 2-Example of system frequency response from raw data

Data samples from the aerodynamic flight-testing system are composed of both dynamic and steady state signals. Many frequency components are present in the raw data. The power spectrum, a measurement of the signal power at various frequencies, is shown in Figure 2. This plot shows the magnitude squared of the DFT in volts^2/Hz. This analysis of a raw data file shows that the majority of elements are concentrated under 120 Hz, although some elements extend up to 450 Hz.

These peaks can vary significantly in amplitude and frequency depending on the test article, test conditions, and the maneuver being performed. Figure 2 shows the frequency response of data taken from the pitch axis sensor of a small cylindrical test article (a simulated fuel tank.) Smaller test articles exhibit a higher frequency response

primarily due to the decreased mass of the model. The aerodynamic properties of the test article can also significantly affect the location and intensity of the observed frequencies.

The data acquisition and processing system operating at the PWT is referred to as the Force and Moment Read-Out System or FAMROS. This system conditions and measures the output of the six-component balance as it is loaded. The resulting data is then stored for future analysis. An in-depth discussion of these balances and the calibration procedure of this system are available in another document "A Minicomputer-Based System for the Calibration of Strain Gage Balances" [1]*.

The dynamic data signal levels can be as large or larger than the embedded steady state data. The dynamic data is monitored to ensure that impulse forces do not exceed mechanical support limits - but the more critical data is the steady state information. Steady state information is derived by filtering the raw input signals with a low pass filter. In the existing configuration, a sequence of analog and digital filters are applied by the FAMROS system. This combination results in a 40 dB reduction of noise power typically set at 4.5 Hz. A more complete description of the existing filtering system is included in Chapter III of this paper.

Figure 3 illustrates raw strain gauge data from the yawing moment measurement axis (shown in blue.) The voltage returned by the balance is proportional to the force measured.

*Numbers in brackets refer to similarly numbered references in the List of References.

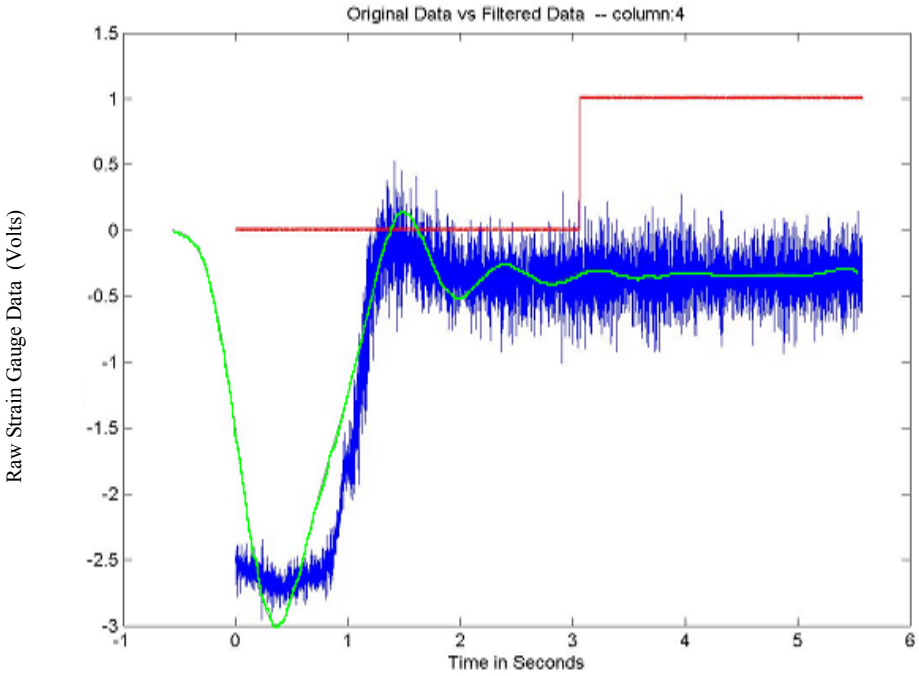

Figure 3-Example of filtered data for the yawing moment measurement

The output of the filter (shown in green) is overlaid on the original data. The red line in Figure 3 represents the system null point which transitions from logic 0 to 1 shortly after 3 seconds. The system null point shows the time that the model positioning system has finished transitioning the model and the next test point is ready for acquisition.

Notice how the blue (raw) data line transitions from –2.5 to 0.0 after one second of acquisition. After the model transition is completed, a damped oscillation is observed in the filtered data. This oscillation represents the control mechanism adjusting the position of the model to reach the desired test point. Once the correct test point is

reached, the system null transitions to logic 1. However, at this point the model position may still be oscillating, and may not be near enough to steady state for accurate data to be taken.

Once this filtered information reaches steady state, accurate force-loading measurements can be accomplished. This information provides the flight performance information that is part of the data product for the customer.

This paper details the approach, process, and the methods used to determine the validity of a real-time stability determination system. Chapter II details the existing acquisition system used in the PWT and the justification for an alternate approach. Chapter III describes the preliminary steps used to acquire raw data from the PWT 4T facility. The frequency analysis of the preliminary data files and the decision to use a 1000 Hz sampling frequency are also discussed.

With the frequency analysis completed, Chapter IV describes the two filter types researched (a 512 point FIR and a 3rd order IIR filter). The IIR filter was the final choice because of the reduction in computational resources required for implementation. Once the filter was chosen, an algorithm was developed to predict the steady state condition of the filtered data. Several candidates were evaluated, but ultimately a method based on a numerical derivative was selected.

Finally, a discussion on a real-time implementation is given in Chapter V with concluding remarks presented in Chapter VI.

CHAPTER II
DEFINITION OF THE PROBLEM

The analog (4-Pole Bessel @ 2 Hz) and digital (2-pole auto-regressive @ 5 Hz, adjustable) filters currently utilized in the existing PWT system impose a requirement to delay data acquisition recording to allow settling of the output data stream to a value within acceptable tolerance levels. Settling time is a function of the high frequency attenuation required and the frequency content of the signals.

A typical test plan involves moving the test model from one position to the next and wait for the data to settle before recording data. Previous data sets have shown that the majority of the dynamic elements of the raw signals will decay within two seconds of the system null 'on position' signal. Since many test programs involve multiple repositions (i.e. a 51-point axial model rotation), even fractions of seconds per point will accumulate to a significant portion of the total testing time.

The data settling time will vary with test article configuration and facility operating condition. The data sample quality will be compromised if it is recorded before the test article has reached steady-state conditions. When this happens for critical data points, additional test time and analysis are required before the test can continue.

The current system utilized in the PWT does not offer an adaptive method of determining the settling time, so the convention is to delay acquisition for a 'reasonable minimum' amount of time to ensure that the test article has settled in a steady state

condition. Unfortunately, this method of additional delay does not eliminate the possibility of recording invalid data sets.

Another issue with this method arises when the data settles before the two-second delay. Some test configurations and conditions can yield a steady state condition well before the two-second delay. The customer will normally accept additional delays to ensure that the dynamic portion of the signal is sufficiently attenuated. However, when each hour of full test plant operation (including all support facilities and personnel) is measured in thousands of dollars – any potential time savings must be pursued.

It is proposed that a system be constructed that will interface to the six-component balance for assessment of settling time before data acquisition. Unlike the main facility recorders, this system will be configured to continuously monitor data during the test. The proposed system will apply signal filtering and sample the same data stream as the facility data acquisition system to provide real-time feedback.

With this type of feedback, the data process controller would be able to determine the ideal time to take the data sample and thus minimize test delay time. These delay times can be the result of either waiting longer than necessary (due to the predetermined settling time) or not waiting long enough for steady state conditions and having to repeat the data measurement.

Each second of testing time at the PWT test cell is a definable cost. Although the research described in this paper is a proof of concept study, it does establish the validity of the approach, which has the potential to save significant time and reduce cost for the Propulsion Wind Tunnel test facilities.

CHAPTER III
APPROACH TO THE PROBLEM

The first step in developing an approach to the problem was to acquire data sets from the PWT test cell. An ideal data series would contain a large variety of raw data sets and would encompass several test articles and test configurations. To allow the use of unclassified test materials, the four-foot wind tunnel (4T) test cell was chosen for this series of experiments. As mentioned in the previous section, the FAMROS system is the data acquisition system used in the 4T test cell. This system was configured to pass the raw input data to the standalone data system unaltered - while ensuring that the data integrity was maintained. Figure 4 is a diagram of the test configuration.

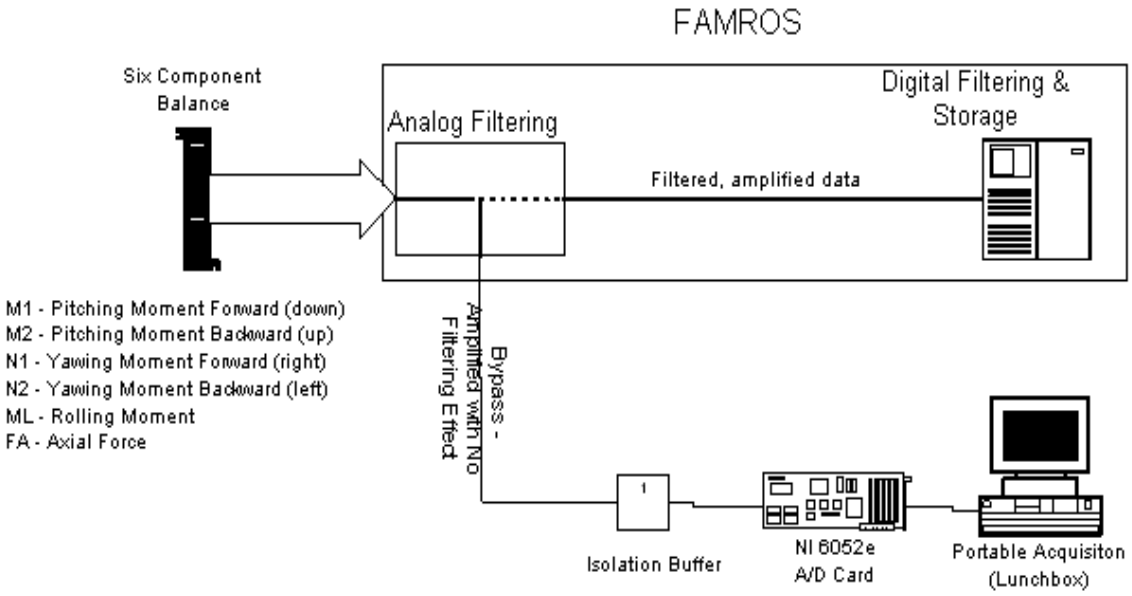

Figure 4 – Block diagram of system configuration

A stand-alone data system (lunchbox computer) was connected in parallel to the existing FAMROS system in order to acquire sample data sets. This lunchbox computer is a portable workstation configured with a National Instruments PCI-6052e data acquisition card. Appendix A details the specific equipment list and configuration. The National Instruments PCI-6052e allows for a sampling rate up to 333k samples per second with 16 bits of resolution. The raw data signal had stress limits of approximately ±7 volts peak. Force monitoring equipment indicated safe operation throughout the test. The 'reasonable' limits for the system were ±5 volts and the data system was optimized for this range.

Custom software was written to allow for flexibility in acquisition. The primary factors to be determined in the acquisition program were signal filtering and data sampling rates. In addition to these, a system null signal was added to the data stream sent to the portable acquisition computer. This signal is a TTL reference signal sent by the test-article positioning system to the FAMROS system to indicate when the model has been successfully moved to the correct test point.

To establish the new approach, the first decision that had to be made was to choose the sampling frequency of the data acquisition system. Since evaluation of new filters was part of this research, the decision of how to sample the raw data was very important. Interviews with PWT personnel indicated that the primary frequency drivers in the raw data correspond to model vibration on the mount and vibration due to the test cell itself. Further talks revealed that the majority of the high-power frequency sources were located below 100 Hz.

Since the predictions indicated the bulk of the high frequencies were below 100 Hz, the first data run included sample rates of 500 Hz, 1000 Hz and 5000 Hz. This range of sampling rates was used to evaluate the correct sampling frequency. Utilizing the Nyquist sampling theory, the 5000 Hz setting would allow for accurate analysis of frequencies up to 2500 Hz. Although the National Instruments card is capable of acquiring data at higher speeds, all predictions indicated that primary drivers should reside well under that frequency.

Table 3.1 shows a chart of the data files acquired, the length of each test, and a brief description of the test article. In the interest of maintaining the minimal level of proprietary information in this document, the test article description is given only in geometric terms. The test articles researched in this paper were all cylindrical objects that will be classified as small, medium or large (S, M, L) in the test description.

Note the smaller articles typically had higher frequency vibrations while the large articles had the larger displacements. However, this was not true for some models that had additional aerodynamic structures mounted on them. These files include several different test model subjects and conditions.

Further acquisitions indicated that although the primary noise drivers do reside at frequencies less than 100 Hz, there are significant peaks above that frequency as well. Figure 5 is a frequency analysis of a raw data set acquired at 5000 Hz. Notice that the majority of the response occurs at less than 500 Hz. Additional data sets verified this behavior for several model types and test conditions.

Table 3.1 – Data Files Acquired with Test Notes

File Number	Name	Sampling Rate (Hz)	Unique Points	Time	Size and Description of Test Article with Test Notes
1/29-a	Data.bin	500	0	8 mins –	Static model (M) – No unique points
1/29-b	Data2.bin	1000	2	5 mins –	cylindrical tank (M) – small movements
1/29-c	Data3.bin	500	1	5 mins –	corrupted file
1/29-d	Mark.bin	1000	3	10 mins-	cylindrical tank (M) – large movements
1/29-e	Mark2.bin	1000	2	5 mins-	cylindrical tank (M) – large movements
1/29-h	Mark12.bin	5000	1	2.5 mins	cylindrical tank (M) – small movements
1/29-i	Mark13.bin	5000	3	3 mins-	cylindrical tank (M) – small movements
2/06-a	Trial1.bin	1000	2	5 mins-	cylindrical tank (S) – large movements
2/06-b	Trial2.bin	1000	2	8 mins-	cylindrical tank (S) – large movements
2/06-c	Trial3.bin	5000	2	3 mins-	cylindrical tank (S) – small movements
2/06-d	Trial4.bin	5000	2	6 mins-	cylindrical tank (S) – small movements
2/18-a	Trial1.bin	1000	2	3 mins-	cylindrical tank (L) – large movements

Table 3.1 – continued – Data Files Acquired with Test Notes

File Number	Name	Sampling Rate (Hz)	Unique Points	Time	Size and Description of Test Article with Test Notes
2/18-a	Trial2.bin	1000	2	5 mins-	cylindrical tank (L) – small movements
2/18-a	Trial3.bin	1000	2	5 mins-	cylindrical tank (L) – large movements
2/18-a	Trial4.bin	1000	2	6 mins-	cylindrical tank (L) – small movements

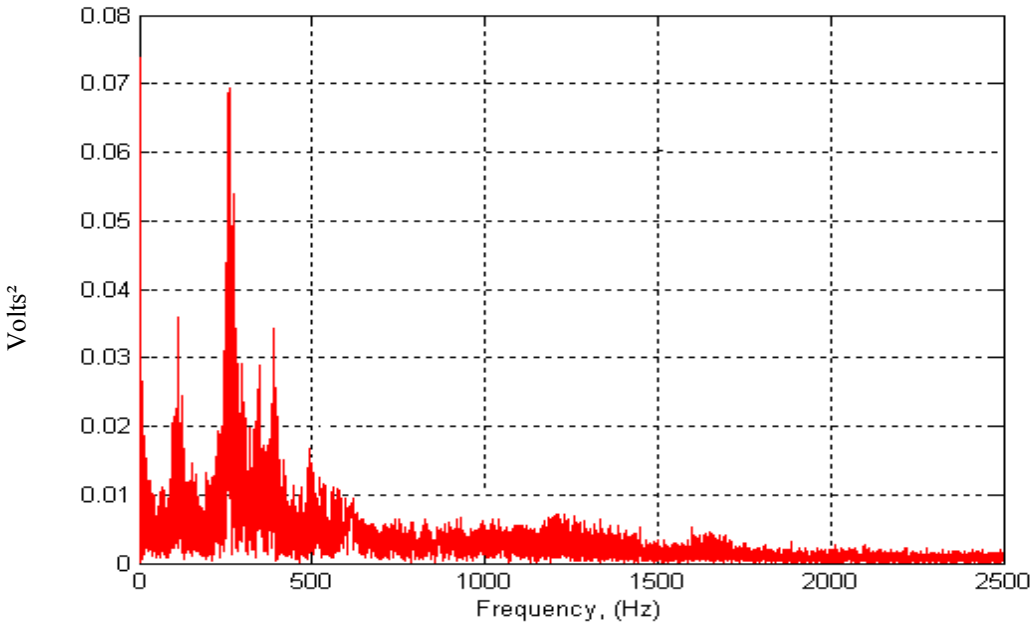

Figure 5 - Frequency plot of signal sampled at 5000 Hz

Some noise continues beyond the 500 Hz, but none with significant power. Because of this determination, the majority of the remaining data sets were taken at 1000 Hz, which easily satisfies the Nyquist requirement of frequency sampling at twice the highest expected frequency. Further verification at 5000 Hz was performed on later acquisitions that included small test articles.

Figure 6 shows a frequency plot for a data set sampled at 1000 Hz. Figures 5 and 6 are representative of all the data sets acquired. Many files had drivers completely under the 100 Hz point and were relatively flat from ~100 Hz out to 500 Hz. Since each data file is different, a frequency analysis was completed on each file to determine the worst case. In addition, all samples classified as worst case were validated with additional data files to eliminate random samples.

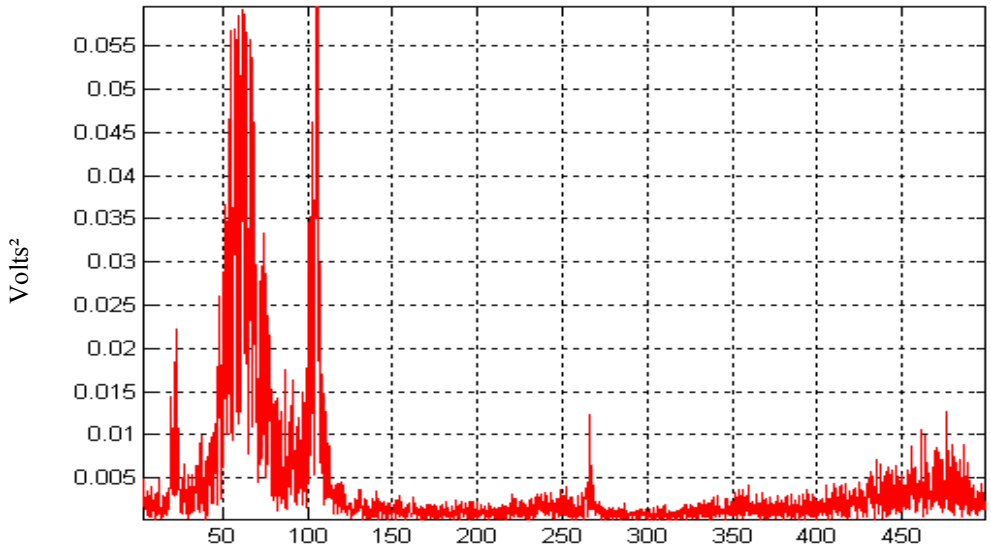

Figure 6 – Frequency plot of signal sampled at 1000 Hz

Once the raw data was acquired, post processing of the data files was performed to isolate areas where the system null pulse transitions from zero to one. This transition indicates that the model has reached its intended position and the FAMROS system is waiting two seconds to take its data point.

Table 3.2 displays a matrix of the individual sample points taken. These axes are referenced as individual data samples. Each axis on the balance is abbreviated with the following acronyms:

M1 - Pitching Moment Forward (relative model motion down)
M2 - Pitching Moment Backward (relative model motion up)
N1 - Yawing Moment Forward (relative model motion right)
N2 – Yawing Moment Backward (relative model motion left)
ML - Rolling Moment
FA – Axial Force

Table 3.2 – Listing of research data elements.

Data Element	Section Number	File Number	Axis	Total Seconds	Scan Rate
1	01/29	marka	MM1	7	1000
2			MM2	7	1000
3			MN1	7	1000
4			MN2	7	1000
5			ML	7	1000
6		markb	MM1	5.5	1000
7			MM2	5.5	1000
8			MN1	5.5	1000
9			MN2	5.5	1000
10			ML	5.5	1000
11		markc	MM1	3.5	1000
12			MM2	3.5	1000
13			MN1	3.5	1000
14			MN2	3.5	1000
15			ML	3.5	1000
16		mark1a	MM1	20	1000
17			MM2	20	1000
18			MN1	20	1000
19			MN2	20	1000
20			ML	20	1000
21		mark1b	MM1	10	1000
22			MM2	10	1000
23			MN1	10	1000
24			MN2	10	1000
25			ML	10	1000
26		mark10	MM1	5	1000
27			MM2	5	1000
28			MN1	5	1000
29			MN2	5	1000
30			ML	5	1000
31		mark10a	MM1	5	1000
32			MM2	5	1000
34			MN2	5	1000
35			ML	5	1000
36		mark11_1K	MM1	4	1000
37			MM2	4	1000

Table 3.2 – continued - Listing of research data elements

Data Element	Section Number	File Number	Axis	Total Seconds	Scan Rate
38			MN1	4	1000
39			MN2	4	1000
40			ML	4	1000
41		mark12	MM1	4	1000
42			MM2	4	1000
43			MN1	4	1000
44			MN2	4	1000
45			ML	4	1000
46		mark13	MM1	3	1000
47			MM2	3	1000
48			MN1	3	1000
49			MN2	3	1000
50			ML	3	1000
51	2/6/2002	trial 1a	MM2	11	1000
52		trial 2a	MM2	9	1000
53		trial 2b	MM1	10	1000
54		trial 2c	MM1	10	1000
55		trial 3a	MM1	10	1000
56		trial 4a	MM2	13	1000
57		trial 4b	MM2	12	1000
58		trial 4c	MM1	12	1000
59	2/18/2002	trial 2	MM2	5.5	1000
60		trial 3	MM1	5	1000
61		trial 3a	MN2	10	1000
62		trial 4	MN2	16	1000

An example of a data file is shown in Figure 7. This file represents a position adjustment with regard to the forward pitching moment (raw data shown in blue.) The output of the filter overlaid on the original data is shown in green. The red line in Figure 7 represents the system null point which transitions from logic 0 to 1 at 3 seconds. The time axis in the following figures is given in relative file time. This file time is identical to the actual test time – with the exception of an offset. The data shows the model position being adjusted during the 0.0 to 2.5 second period and ready to take data after the three-second point. The time between 2.5 and 3 seconds is the stabilization time of the system.

Notice how the null position indication occurs at three seconds (relative sample time.) Using current algorithms, the FAMROS system will wait until the five-second mark (relative sample time) before considering the system stable enough for taking data.

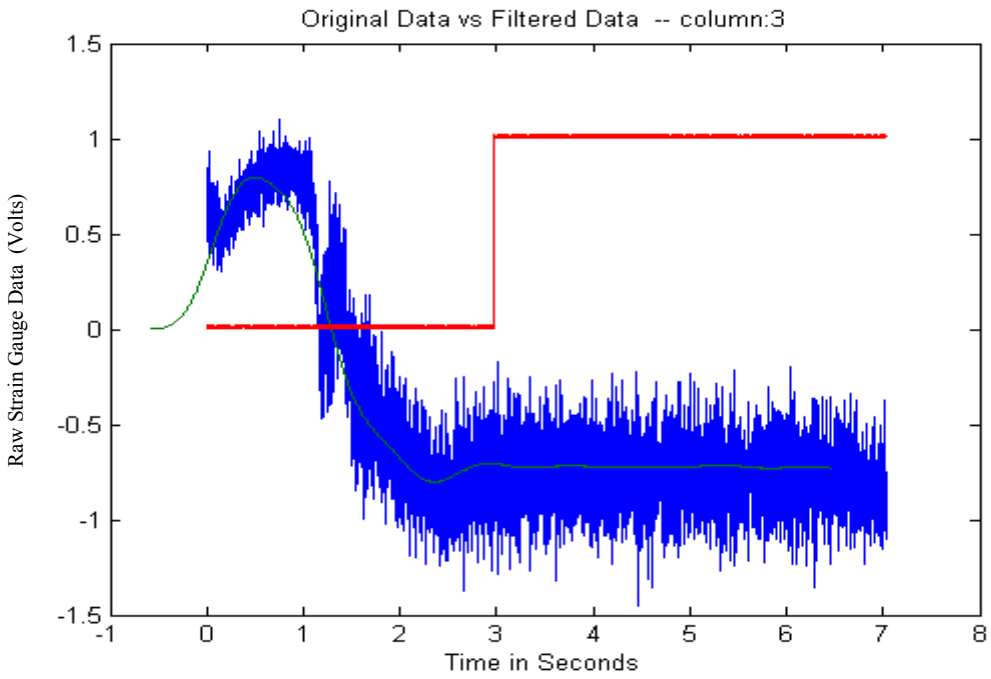

Figure 7-Pitching Moment Forward (relative model motion down)

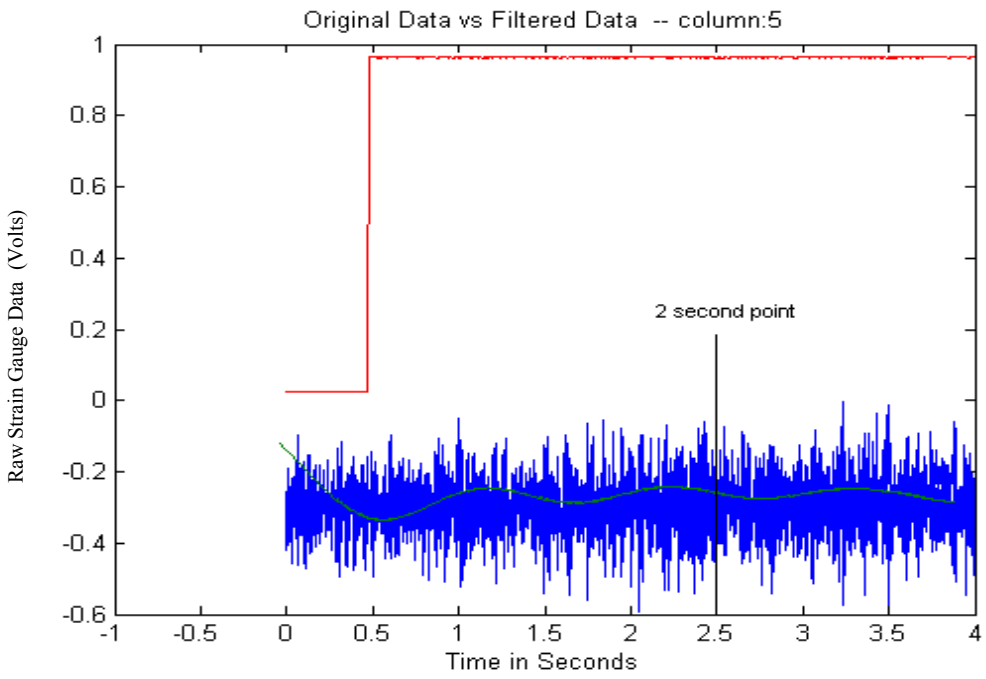

Figure 8 - Yawing Moment Forward (relative model motion right)

In the next case (Figure 8), the data file shows the system null at 0.5 seconds. Notice that the filtered data (shown with green line) still oscillates after the 2-second point (shown with black line.)

Depending on the sensitivity of the measurement, the oscillation in Figure 8 might not be excessive enough to prevent a valid data acquisition point. This determination is made by the test coordinator and ultimately, the test client. The current test configuration (using the FAMROS data acquisition system) does not monitor the balance output for data stability. Analysis of historical data indicates that most test configurations achieve stability within two seconds after system null. However, as the preceding Figure 8 shows, some data sets require more time to achieve steady state.

CHAPTER IV
THE RESEARCH RESULTS

As described in the previous chapter, the raw data sets were acquired, analyzed for frequency content, and sub-divided into smaller areas of interest. These areas were chosen to include regions where the system null pulse was in transition from low to high. This transition indicated the model positioning system had completed moving the test article and the FAMROS system was awaiting the two-second pause before the data acquisition.

In Chapter III, a discussion of the frequency analysis showed that the majority of the signal information resides below the 500 Hz threshold. Even when the signal is sampled up to 5000 Hz, no additional large frequency components were found. Since this determination, all the source data files were acquired or re-sampled at 1000 Hz. Files acquired in later acquisition runs at the test cell were sampled at 5000 Hz when the system model was changed or the test conditions were significantly altered.

These test files were subsequently evaluated and the frequency analysis verified that all the primary signal drivers present were below the 500 Hz point. All further analysis was performed on data sampled at 1000 Hz.

With the raw data frequencies identified, the next step was to identify the type of filter and the filter parameters that would remove all the high frequency information, while retaining the low frequency (less than 5 Hz) information. The low frequency

information is necessary to determine if the oscillation of the test model has decayed below a preset limit.

Several types of filters were evaluated for this project. The first goal was to analyze the existing filter architecture used in the test cell. Since the balances are extremely low voltage devices, the output signals require amplification and conditioning to enable satisfactory digitization. Currently, the PWT 4T test cell uses a 50 channel Pacific Instruments integrated signal conditioner/amplifier to interface the raw balance data to the A/D converters. The amplifier section of this unit has a 4-pole Bessel low pass filter with selectable cutoff frequencies. The total filter system response is selectable, but is normally set 3dB down at 1.5 Hz and 40 dB down at 4.5 Hz.

The purpose of this research was to determine a method that could report to the test stand when a test article had achieved a steady state condition (as defined by pre-determined balance data uncertainty calculations.) The research was pursued with the understanding that the prediction algorithm would receive unfiltered, raw data from the measurement balances. This would allow for variations in either system (filtering, sampling, etc.) without adversely affecting the data acquisition system.

The first step in this process was to determine a filter type that could simulate the performance of the existing analog/digital filter system. This filter would need to be realizable in software for later inclusion in a digital signal processor (DSP) or standalone computer system. Several filter designs were evaluated; the first was the finite impulse response filter (FIR.) This filter design was accomplished following the design

procedure outlined in several Digital Signal Processing textbooks for the design of an Equiripple FIR filter [2].

The FIR design makes use of the Parks-McClellan computer program, which uses the Remez exchange algorithm to determine the filter impulse response. In order to achieve the 40 dB attenuation at 4.5 Hz, while restricting the ripple to 2 percent, a filter order of 512 was needed. The specifics for this filter are:

Filter Type: Low pass, Linear Phase

Band	Lower Edge	Upper Edge	Gain	Weight
1	0.0000	0.0020	1.0000	1.0000
2	0.0065	0.5000	0.0000	1.0000

The filter's response is shown in Figure 9. The coefficient file for this filter is attached in Appendix B.

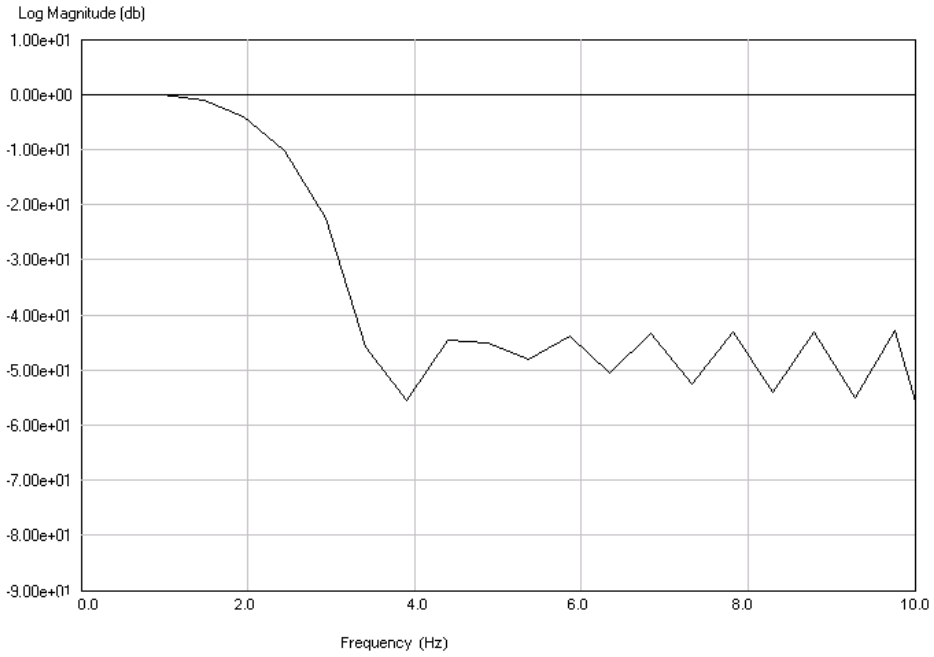

Figure 9 –Frequency response of FIR filter.

In order to filter the incoming raw data, a coefficient file is specified and read by the acquisition program. The program allows the user to select a specific filter by choosing a specific coefficient file. Once this file is selected, the program processes the incoming data with the filter defined by the impulse response coefficient file. Details on this new acquisition program are given in Chapter V.

The equation below shows the programmatic FIR filter implementation.

$$y(n) = h(0)* x(n) + h(1)*x(n-1) + \ldots + h(k)*x(n-k)$$

Further research showed that a better result could be achieved using an infinite impulse response filter (IIR.) The advantages of this filter include a more stringent frequency response characteristic with a much lower order difference equation. A reduction in the filter elements also reduces the computational resources needed for filter implementation. This advantage increases the number of platforms that can support the final implementation.

The primary disadvantage of this type of filter is the possibility of creating an unstable system. This can be prevented by ensuring that the filter poles are inside the unit circle.

Using the same band edges specified in the FIR filter design, several IIR filters were implemented. The goal of this study was to compare the results of both types of filters using the same raw data sets.

The next step was to apply this filter programmatically to the same raw data sets evaluated with the FIR filter implementation. The IIR filter was achieved with the following algorithm [3] that was implemented in the acquisition program (described in Chapter 5 – Real-time Implementation.) The filter is a "Direct Form II Transposed" implementation of the standard difference equation:

y(n) = b(1)*x(n) + b(2)*x(n-1) + ... + b(nb+1)*x(n-nb)
- a(2)*y(n-1) - ... - a(na+1)*y(n-na)

…where max{na,nb} is the filter order

The filter was designed using the ELLIP.M function included with the MatLAB 6 distribution. The function designs an Nth order lowpass filter with user specified parameters for ripple, order, stopband, and stopband attenuation. The coefficient list for this filter is included after the FIR coefficient list in Appendix C. The parameters used for this program were as follows:

Order: 3
Filter: Lowpass — Filter Type: Elliptic
Band Edge Freq 1 : 0.0020 — Band Edge Freq 2: 0.0065
Passband Ripple (dB): $4e^{-2}$ — Stopband Attenuation (dB) 40

Note: Band Edge Definition $= \frac{fc}{fs}$

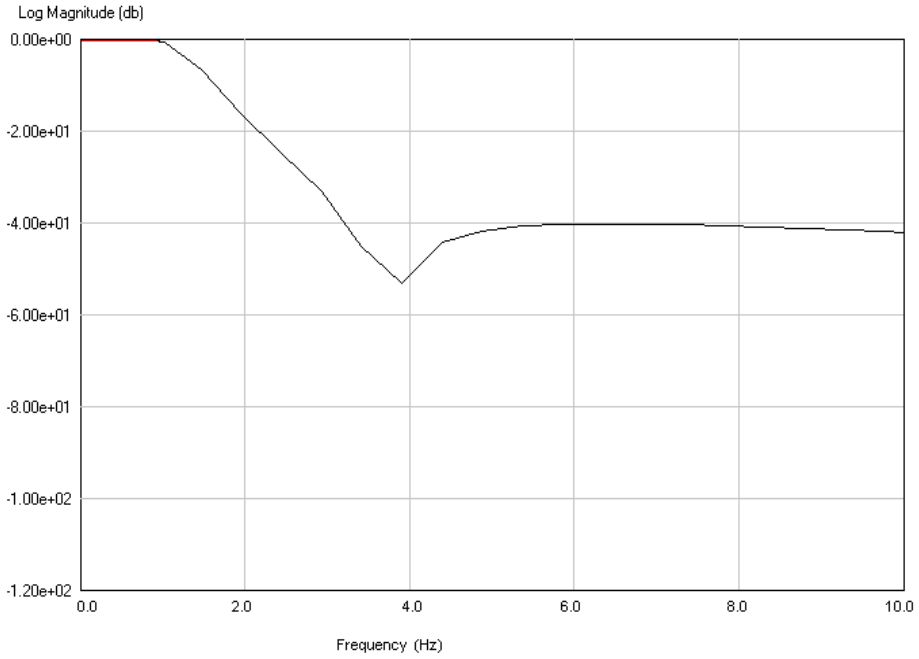

Figure 10 – IIR Filter response

Figure 10 shows a graph of the IIR filter frequency response. This figure plots filter response in log magnitude from zero to 10 Hz.

Once this filter was implemented in software, the raw data sets were re-processed. One result is shown in Figure 11. Notice the red vertical line at 0.5 seconds. This is the system null pulse indicating that the model positioning system has finished moving the test article. The blue 'noise' is the raw, unfiltered data signal. The green line is the result of the IIR filter application overlaid on the same x-axis as the raw signal data. The FIR filter implementation had a similar result – but required significantly more computer resources for computation

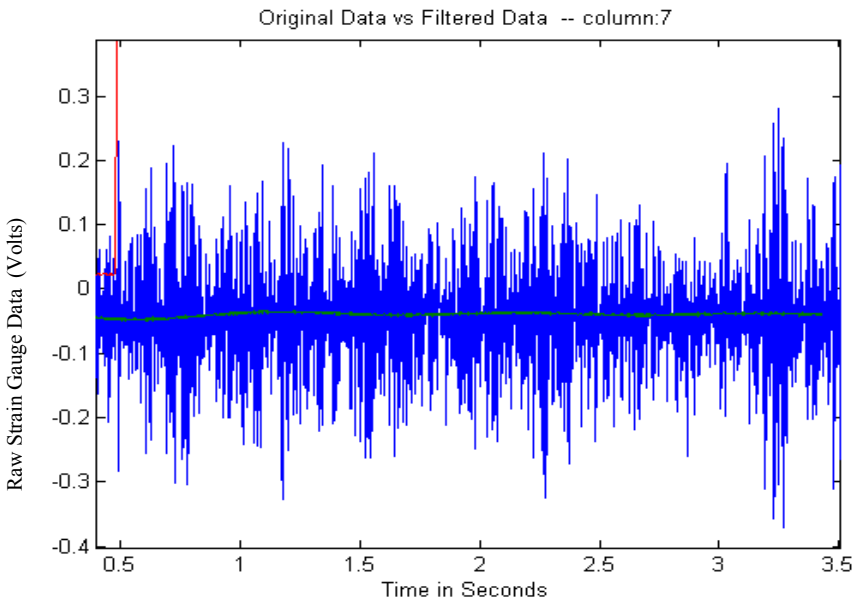

Figure 11 – Raw data filtered with IIR filter

The group delay of the IIR filter ranged from 190 to over 300 samples in the filter pass band (using the GRPDELAY.M function in MatLAB) whereas the delay for the FIR filter was 255 samples. The FIR filter delay was determined by:

(# of Taps-1)/2=255 samples *Taps=512*

The larger, variable delay of the IIR filter does not equate to a disadvantage. Because the proposed implementation of these filters calls for continuous operation during a test sequence – after the initial pre-loading, the filter delay does not factor into system performance. In addition, these delays still measure less than 0.3 seconds at the proposed sampling rate, which is negligible with respect to the test cell model motion.

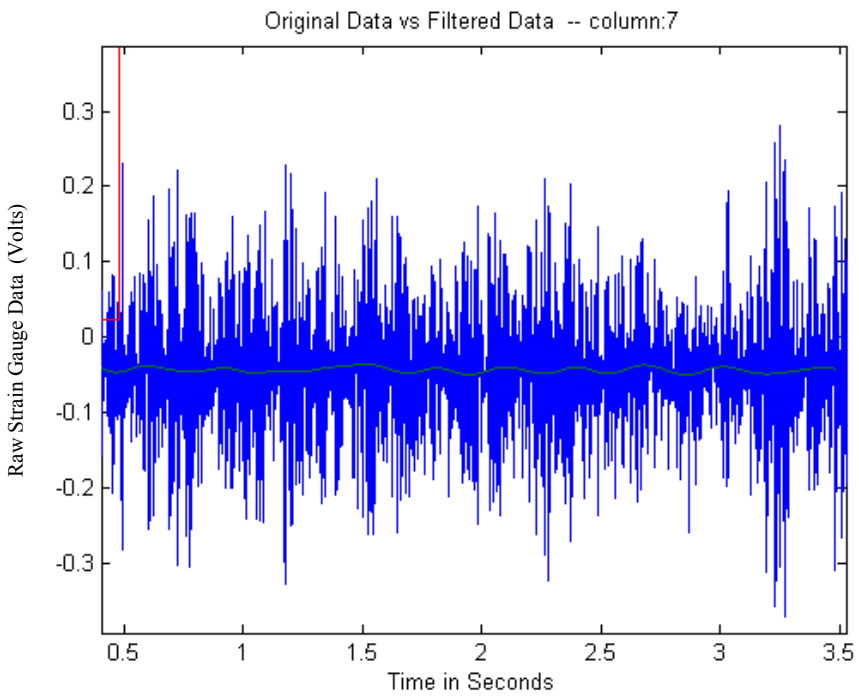

Figure 12 – Raw data filtered with FIR filter

Figure 12 shows the exact same data set filtered with the FIR filter. Notice the filter output has higher frequency oscillations than the same file filtered with the IIR filter (shown previously in Figure 11).

While the noise has been greatly attenuated with the FIR filter implementation, the result is not as smooth as the IIR implementation. The primary reason for this variance can be attributed to the roll-off differences between the filters. Referring to Figure 9 (FIR filter) and Figure 10 (IIR filter) as discussed previously, the IIR filter exhibits a faster roll-off than the FIR implementation, which results in more attenuation of the signal at lower frequencies.

Another feature of the IIR filter is the steadily increasing stop band attenuation. The FIR filter provides a constant attenuation of –40 dB starting at 4 Hz. The IIR filter attenuation starts from –40 dB at 4 Hz and increases to –80 dB at 440 Hz. This additional attenuation further decreases the effects of high frequency noise.

Ultimately, the IIR filter was chosen based primarily on its more efficient implementation. This filter would require fewer system resources to implement in an embedded design.

Once the filter type and implementation were selected, the next step was the development of an algorithm that could provide a measure of stability. Several approaches were evaluated, but ultimately two were selected for comparison trials: the relative difference method and the derivative method.

Each method was evaluated on three points: accuracy, repeatability, and the time of determination. The accuracy was determined by comparing the result of the algorithm with a visual judgment of settling. Repeatability was measured by testing the same data file in at least three separate locations and comparing the results. The final test was the time of determination. This test was the earliest time, after the system null, that the algorithm called a tentative steady state.

The visual judgment test is the reference time point when the post-filtered data appears to be settled. Since no absolute stability point exists for this data, a visual analysis of the data is required. Ideally, this visual analysis should be performed by an aerospace engineer who is familiar with the test article, facilities, and conditions. Though this type of analysis was not feasible for this study, a uniform method of evaluation was

developed and applied to all the data samples in order to determine this reference time point.

The evaluation method required that all the data samples be displayed on the same axis scale. Since this analysis was performed with offline data, an entire timeline (5-15 seconds of data) could be displayed. This allowed for the observation of damped-oscillations and other trends that revealed potential stability points. Once these points were identified, they were examined for duration. If these potential stability points remained valid for one second, they were judged valid stability points and the numerical methods were compared to these points.

The relative difference method was implemented by examining subsequent filtered data points and comparing the difference to a running average of the previous (m) values.

The equation used for this method is as follows:

$$\Delta_n = \frac{Y_n - Y_{(n-1)}}{\frac{1}{(m-1)} \sum_{i=n-m}^{n-2} Y_i}$$

Condition: Δ_n = (Tolerance value: K)
For 250 successive values.

The value of m was chosen to maximize the algorithm response time while ensuring the closest match to the stability point determined by visual inspection. Preliminary values chosen were integers from 3 to 25. Values less than 10 were

discarded primarily because the result never settled to a potential stability point. The algorithm result for these cases would fluctuate constantly between true and false cases.

Values of m larger than 10 delayed the algorithm judgment further from the 'visually judged' stability point. No points higher than 25 were used since the data trend became apparent as m approached 20. The value that returned the closest results to the 'visually judged' stability point was experimentally determined to be 10. All the data files were evaluated with m equal to 10. However, as test conditions changed, m was re-evaluated to ensure that the algorithm output was returning the best result.

The algorithm response time of 250 points (one quarter second at the sample rate of 1000 Hz) was deemed sufficient for this project. The tolerance value (K) was chosen to be 0.001. Larger values of K were tried, but in experimental trials the algorithm returned too many false positives.

A graph of the algorithm output is shown in Figure 13. The blue line represents the output of the IIR filter after the system null indicated that the model has finished its transition. The red line represents the output of the relative difference algorithm. When the pulse is in the true state, the algorithm is returning a potential steady state point.

Two conditions were required for the relative difference method to assert a tentative steady state condition. First, the system null pulse was required to be in a true state. This signaled that the model positioning system had completed the movement operation. Second, the difference between successive points must steadily decrease to a user selectable tolerance value (K). Once below the tolerance value, the difference would be required to remain below that value for 250 data points.

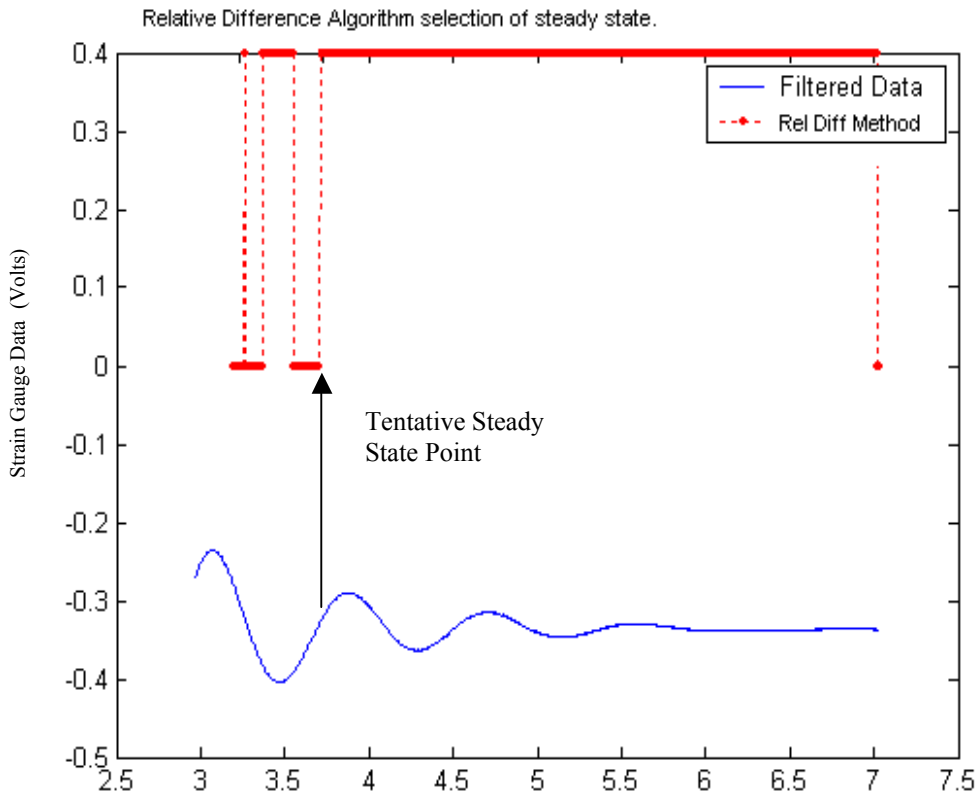

Figure 13 – Relative difference method evaluation after Null asserted

Notice the oscillations in Figure 13 before the 3.7-second point. These oscillations are not valid stability candidates since they do not remain true for the required quarter second. A potential true condition returned by this algorithm occurred at 3.7 seconds.

All the data sets were evaluated with the relative difference method with good results. Most of the files returned a steady state condition around the two-second mark. A table showing the test results and a comparison of both methods is shown after the next section, which describes the derivative method.

The second method of steady state evaluation is called the derivative method. This method utilizes the numerical derivative by examining 'the rate of change' of the filtered data stream. The output of this algorithm is equal to the slope of the line tangent to the displacement vs. time. The algorithm used is shown in the equation below.

$$\left(\frac{Y_n - Y_{(n-1)}}{\Delta t} \right) \leq K$$

K = Tolerance for 250 successive values. Δt = sample spacing.

The algorithm measures the change of slope of the filtered data with respect to time and monitors the result as it trends to K. As the derivative value decreases below a pre-set tolerance value (usually set close to zero, 0.001 for the current research), a tentative steady state is located in the data stream. The tolerance value is adjusted during analysis to ensure that the algorithm is returning the best results.

If the duration of the tentative steady state signal exceeds one-quarter of a second (maintaining the comparison with the relative difference method), the algorithm asserts a steady state true signal. This condition is also dependent on the condition of the system null pulse. If the null pulse is in a false condition, the algorithm will not assert true. Figure 14 shows a graph of the derivative method algorithm applied to the same data set used for the relative difference discussion.

The filtered data is displayed in blue, and the steady state determination returned by the algorithm is shown in red.

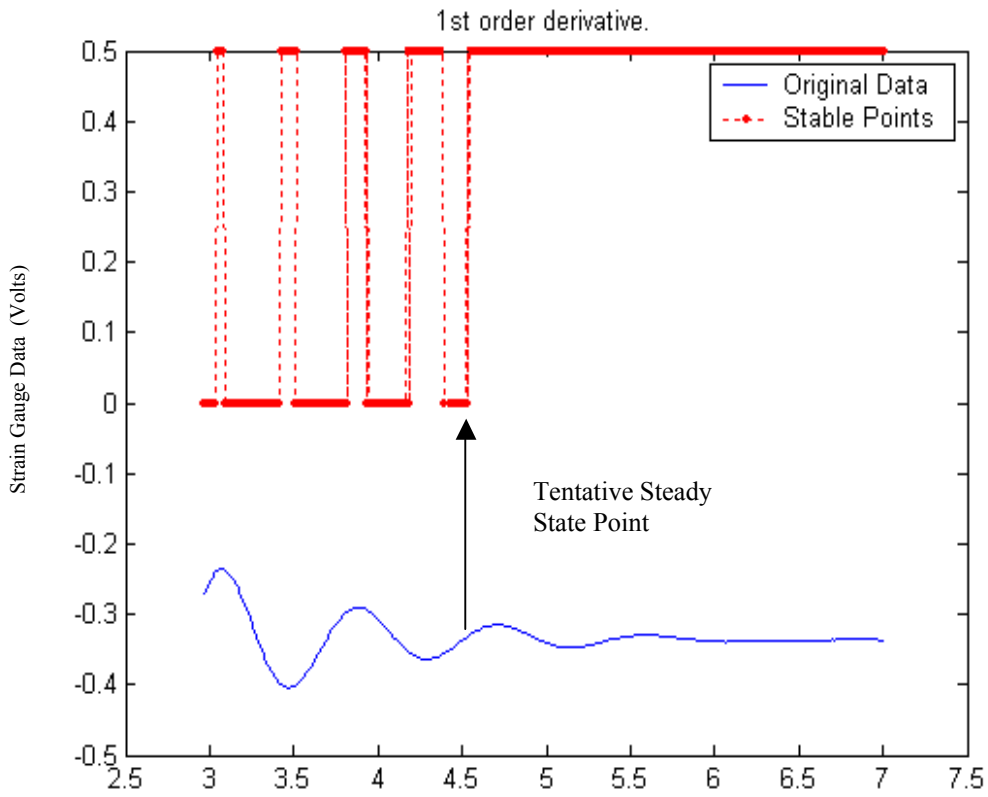

Figure 14 – Derivative Method applied to IIR filtered data

The algorithm returns a possible steady state point at the 3.1, 3.5, 3.7 and 4.1 second marks – but these are not valid because the duration is not long enough (250 samples, one quarter second.) The valid true occurs at the 4.5-second mark (which is still a half second less that the existing 2 second delay.) Notice, however, the relative difference method returns a true condition at the 3.7-second mark. Visual examination of the raw data at this point reveals un-settled data. As mentioned earlier, a visual analysis by an aerospace engineer who is familiar with the test article, facilities and conditions should make this determination. However, a uniform method of evaluation was

developed and applied to all the data samples in order to determine this reference time point.

The following table (Table 4.1) lists the results of both algorithms in comparison to what was determined by visual inspection. The reader should reference Figure 15 immediately following the table for a description of the symbols used in the table.

The derivative algorithm yielded better results than the relative difference method. As shown in Table 4.1, the number of false true conditions was greatly reduced. The accuracy in comparison to the visual inspection method also improved with the derivative method. The relative difference method was evaluated multiple times in order to fine-tune the adjustable parameters. The results presented in this paper represent the parameters that returned the best results.

The derivative method is superior to the relative difference method both experimentally and in actual implementation. The relative difference method has an additional averaging factor (m - currently set to 10) that needs more adjustment than the derivative method, which utilizes the slope calculation to determine steady state.

The derivative method is also easier to implement in modern DSPs due to the inclusion of the standard derivative function. This is in contrast to the sequences of additions, subtractions, and divisions that the relative difference method utilizes. In addition, with fewer 'tunable' parameters, the derivative method requires less user input for operation. This simplifies the final user interface.

Table 4.1 – Comparative Results of Steady State Algorithms

Data Element	File Number	Axis	Total Seconds	Visual Judged Method	Relative Difference Method - A	Derivative Method - B	Closest to Visually Judged
1	marka	MM1	7	0.50	*0.25	0.50	B
2		MM2	7	1.00	1.00	1.00	-
3		MN1	7	1.00	0.75	0.75	-
4		MN2	7	1.50	*0.75	1.50	B
5		ML	7	0.75	0.75	1.00	A
6	markb	MM1	5.5	0.25	0.50	0.25	B
7		MM2	5.5	0.75	0.50	0.75	B
8		MN1	5.5	0.75	*0.50	0.75	B
9		MN2	5.5	0.75	0.75	0.75	-
10		ML	5.5	0.75	0.75	0.75	-
11	markc	MM1	3.5	0.60	0.40	0.60	B
12		MM2	3.5	1.00	X	0.90	B
13		MN1	3.5	1.20	1.00	X	A
14		MN2	3.5	1.00	X	0.90	B
15		ML	3.5	1.20	X	1.90	B
16	mark1a	MM1	20	1.50	X	1.60	B
17		MM2	20	1.20	1.20	1.25	A
18		MN1	20	2.00	2.00	2.00	-
19		MN2	20	2.00	1.75	1.75	-
20		ML	20	2.00	*1.75	2.00	B
21	mark10	MM1	5	1.75	*1.00	1.75	B
22		MM2	5	0.75	0.75	0.75	-

Table 4.1 –continued – Comparative Results of Steady State Algorithms

Data Element	File Number	Axis	Total Seconds	Visual Judged Method	Relative Difference Method - A	Derivative Method - B	Closest to Visually Judged
23		MN1	5	1.25	1.50	1.25	B
24		MN2	5	1.25	1.25	*1.00	A
25		ML	5	0.75	1.00	0.75	B
26	mark10a	MM1	5	1.25	1.00	1.25	B
27		MM2	5	1.25	*0.50	1	B
28		MN1	5	2.00	*0.75	1.75	B
29		MN2	5	1.25	1.00	1.25	A
30		ML	5	0.50	0.75	0.50	B
31	mark11_1K	MM1	4	2.25	*1.25	2.00	B
32		MM2	4	1.25	X	1.00	B
33		MN1	4	2.25	*1.75	*1.75	-
34		MN2	4	2.25	2.00	2.50	A
35		ML	4	2.25	2.00	2.25	B
36	mark12	MM1	4	1.25	1.75	1.50	B
37		MM2	4	1.50	X	1.25	B
38		MN1	4	1.25	X	1.00	B
39		MN2	4	1.50	X	1.50	B
40		ML	4	1.00	X	1.25	B
41	mark13	MM1	3	0.50	0.50	0.50	-
42		MM2	3	0.50	0.50	0.50	-
43		MN1	3	0.50	0.50	0.50	-
44		MN2	3	1.25	1.25	1.00	B
45		ML	3	1.00	1.25	1.00	B

Table 4.1 –continued – Comparative Results of Steady State Algorithms

Data Element	File Number	Axis	Total Seconds	Visual Judged Method	Relative Difference Method -A	Derivative Method - B	Closest to Visually Judged
46	trial 1a	MM2	11	1.00	X	1.00	B
47	trial 2a	MM2	9	2.25	*0.25	2.00	B
48	trial 2b	MM1	10	2.00	2.00	2.25	A
49	trial 2c	MM1	10	2.00	1.50	1.50	-
50	trial 3a	MM1	10	1.00	0.50	0.50	-
51	trial 4a	MM2	13	2.00	1.80	2.00	B
52	trial 4b	MM2	12	1.50	1.75	1.50	B
53	trial 4c	MM1	12	1.00	1.00	1.00	-
54	trial 2	MM2	5.5	0.25	X	0.25	B
55	trial 3	MM1	5	0.75	1.00	1.00	B
56	trial 3a	MN2	10	0.75	0.75	0.50	A
57	trial 4	MN2	16	1.00	X	1.00	B
58	trial 4a	MM1	11	1.00	0.75	0.75	-
59	trial 4b	MN2	15	1.00	1.00	1.00	-

‘*’ - This symbol was used to mark times that looked incorrect. The algorithm made an assertion that did not agree with the Visually evaluated method.

‘X’ – This symbol represents a non-conclusive result. The algorithm was unable to make a determination.

‘-‘ – This symbol represents a tie score – both algorithms chose the same time.

Figure 15 – Symbols used in Table 4.1

Table 4.2 –End Results of Steady State Algorithms

59 total data points	**Closest to Visually Judged 'win'**	**Not closest to Visually Judged 'lose'**	**Tie Scores**	**Inconclusive**	**Total Incorrect**	**TOTALS**
Relative difference Method	8	**13**	16	**12**	**10**	59
Derivative Method	**35**	5	16	1	2	59

The results of the comparison between the relative difference method and the derivative method are summarized in Table 4.2. The highest numbers are emphasized in bold type. The stability time returned by each algorithm is compared to the visually determined stability point for each data element. The algorithm that returned a closer match to the visual determined point was judged a 'winner' for that data point. On several occasions, both algorithms matched the visual determined point. This was noted as a 'tie' in Table 4.1. If the algorithm was unable to return a potential steady state point for a data set, the result was declared 'non-conclusive.' Finally, if the algorithm returned an incorrect stability point, it was labeled 'incorrect.'

As shown in Table 4.2, the derivative method scored much higher than the relative difference method on total 'wins' as well as minimal 'non-conclusive' and 'incorrect' results.

CHAPTER V
REALTIME IMPLEMENTATION

In the previous chapter, the derivative method of stability prediction and the infinite impulse response (IIR) filter implementation yielded the best results for determining the steady state condition of the testing model. The final step in this research was to implement both the filter and the determination algorithm on a data acquisition machine and observe whether the machine could determine the steady state nature of the test article.

Early in the research phase, the data acquisition program was modified to evaluate different ways of applying filters to the raw data. The program was designed with a modular architecture to allow for the inclusion of separate processing components without a major rewrite effort. The first filter type to implement was the FIR (finite impulse response) filter. Several test runs were completed using this filter type to verify the capability of the filter in a 'live' monitor mode during a live PWT test. Since later research described in Chapter IV showed the IIR filter gave better results, the acquisition program was revised to run with the IIR filter. The data system was configured identically to the system described in Chapter III with respect to hardware and external configuration.

The user interface shown in Figure 16 was initially developed for the acquisition system and was modified to implement the active filtering algorithm. The filters are chosen before the acquisition run by selecting the **setup** function.

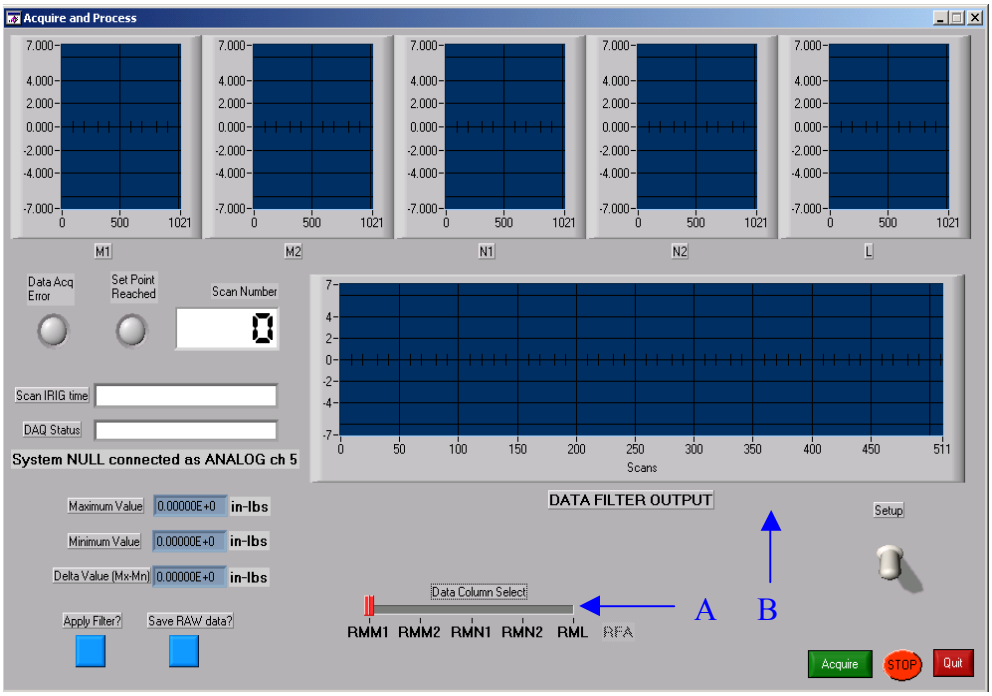

Figure 16 – User interface for acquire program with active filtering.

Figure 16 shows the new user interface of the acquisition program. Note the selector bar (**A**) in Figure 16; this control selects which channel is filtered and displayed on the Data Filter Output screen (**B**.)

A block diagram describing the operation of the new program is shown in Figure 17. This diagram represents the original code as modified to filter the incoming data. After the NI card is initialized, the user has the option to save the raw, unfiltered data directly to the storage device (hard drive.) If the user wants to apply a digital filter to the data stream, the program prompts the user for a data file that contains the coefficients of the desired filter. Once the data is acquired and stored, the program resets to allow for additional acquisitions. The program configuration is handled by a separate control shown in Figure 18.

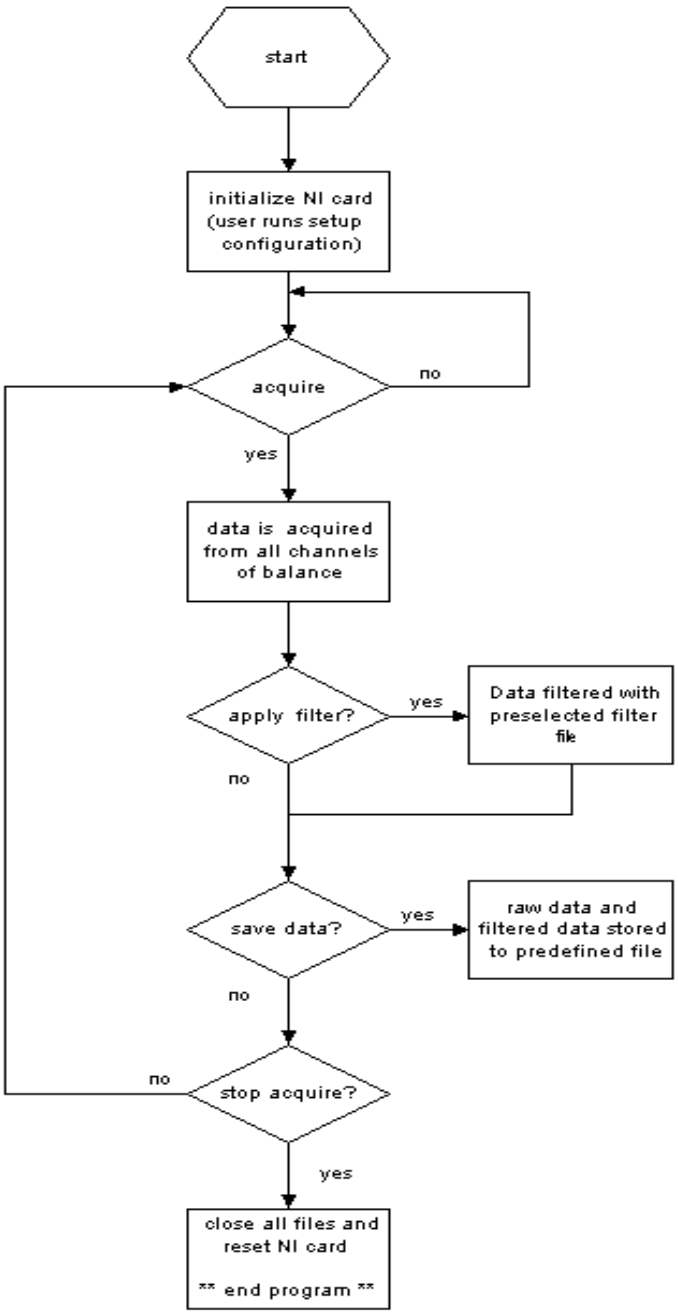

Figure 17– Flowchart of acquire program with filtering option.

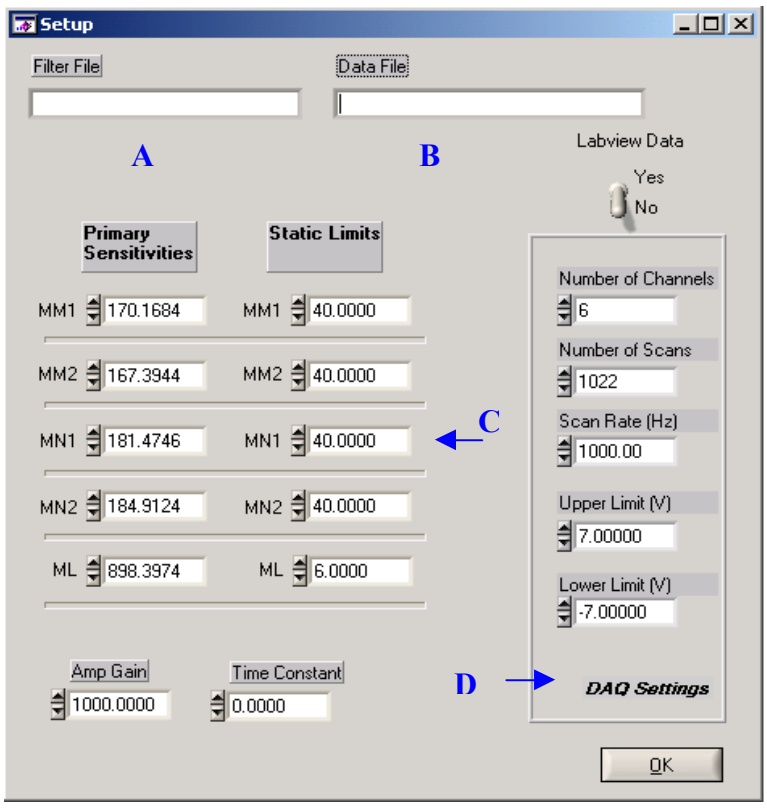

Figure 18 – Setup control for acquisition program

The program setup screen (Figure 18) allows for the selection of various pre-determined IIR filters (**A**) to be used in the on-line monitor mode. The Data File dialog box (**B**) allows the selection of the output name and directory for the data files. The parameters for the National Instruments acquisition card are chosen in the DAQ Settings field (**D.**) The Static Limit fields (**C**) are calibration constants for a future version.

The filtered data acquired with this system was compared with the results of the 'off-line' post-processing program. A frequency analysis of post-processed data and the output of the 'on-line' filter showed similar results with no high frequency components. A frequency analysis of these two curves is shown in Figure 19.

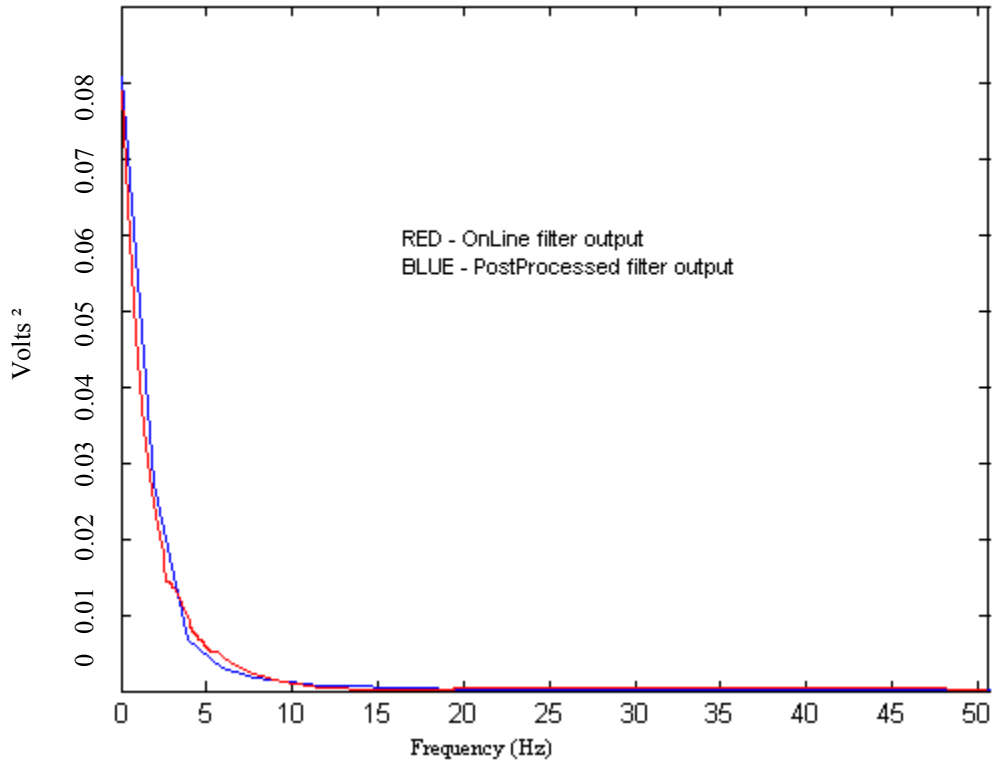

Figure 19 –Frequency analysis comparison between online and offline filtering

The frequency responses shown in Figure 19 are representative of additional analysis completed on both post-processed and online filtering. The slight variations are due to changing test conditions (model orientation and tunnel conditions were not identical between each acquisition series).

The next step in validation testing was the implementation of the stability algorithm into the acquisition program. As discussed in Chapter IV, the derivative algorithm had the best results and used less computational resources. Once the specific filter coefficients are selected, the algorithm returns a Boolean true or false to reflect the

stability of the data input to the system. This system is also dependent on the system null signal from the FAMROS system. This null signal in conjunction with the stability predication algorithm will reflect the quality of data indicator to the facility test system.

The acquisition program was modified to allow for this processing to occur immediately after the data passes through the IIR filter. The user selects a file containing the IIR filter coefficients. The intended operation of this program allows for flexibility in filter selection (pass-band, stop-band, and attenuation) in order to optimize the filter type for a particular test article. Figure 20 shows the software flowchart modified with the new code.

With these modifications, the acquisition program was adapted to make steady state determinations of raw balance data. This revision has been implemented and tested with simulated inputs. The simulation involved combining the output of a function generator and a white noise generator [4]. This configuration allowed an approximation of an actual balance output.

The results mirrored those of the off-line predictor that was described in the previous chapter. Table 5.1 below shows the composite algorithm (IIR filter implementation with the derivative method) in comparison to the visual inspection (visually judged method.)

Please note that the listed times are relative to the system null pulse. The existing FAMROS system took a data point at relative time 2.0 seconds.

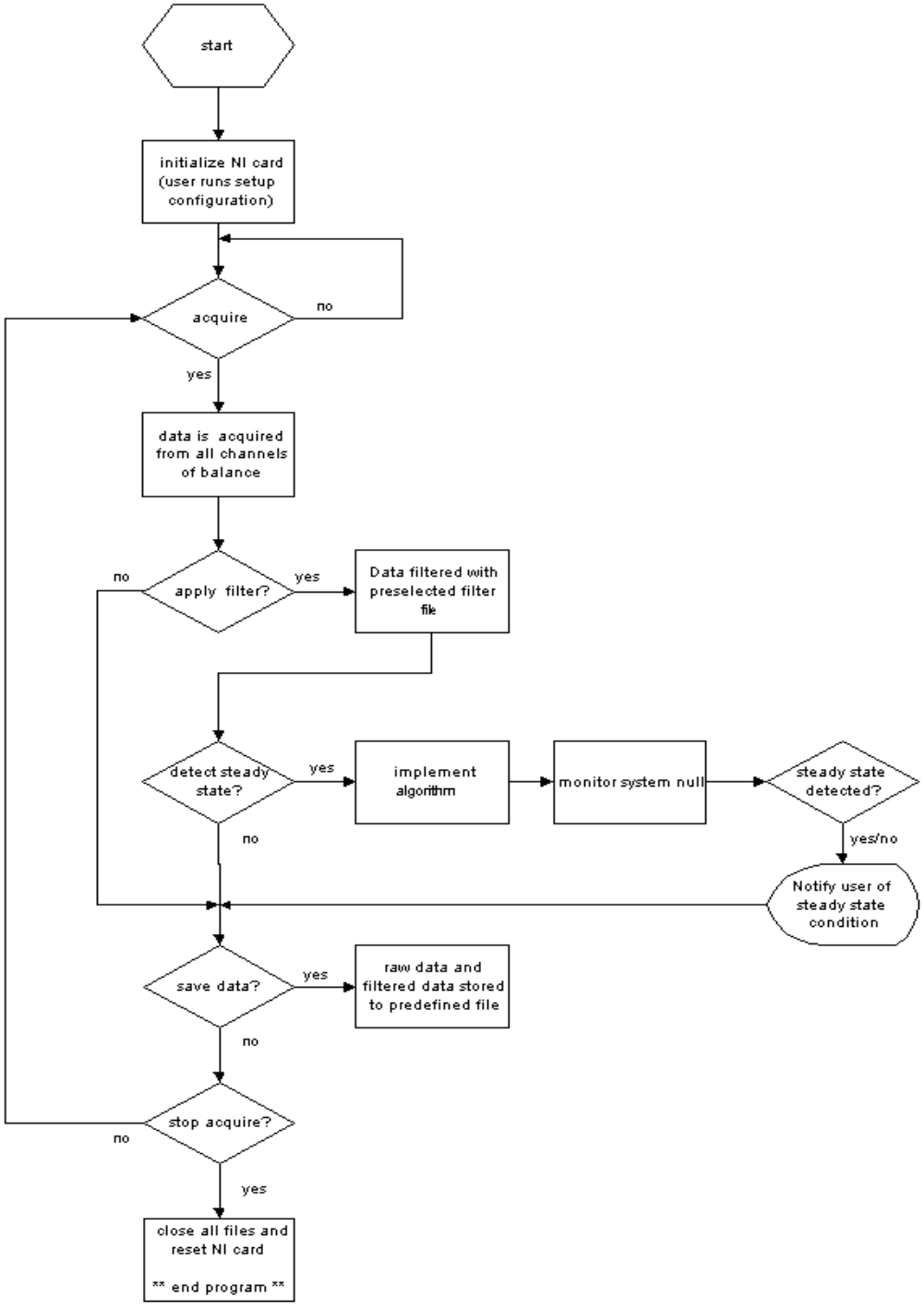

Figure 20 – Modified data acquisition program with analysis

Table 5.1 – Composite Algorithm Measured in Relative Time

Data Element	File Number	Axis	Visually Judged Method	Derivative Method with IIR Filter
2		MM2	1.00	1.00
3		MN1	1.00	0.75
4		MN2	1.50	1.50
5		ML	0.75	1.00
6	markb	MM1	0.25	0.25
7		MM2	0.75	0.75
8		MN1	0.75	0.75
9		MN2	0.75	0.75
10		ML	0.75	0.75
11	markc	MM1	0.60	0.60
12		MM2	1.00	0.90
13		MN1	1.20	Non-conclusive
14		MN2	1.00	0.90
15		ML	1.20	1.90
16	mark1a	MM1	1.50	1.60
17		MM2	1.20	1.25
18		MN1	2.00	2.00
19		MN2	2.00	1.75
20		ML	2.00	2.00
21	mark10	MM1	1.75	1.75
22		MM2	0.75	0.75
23		MN1	1.25	1.25
24		MN2	1.25	1.00
25		ML	0.75	0.75
26	mark10a	MM1	1.25	1.25
27		MM2	1.25	1.00
28		MN1	2.00	1.75
29		MN2	1.25	1.25
30		ML	0.50	0.50
31	mark11_1K	MM1	2.25	2.00
32		MM2	1.25	1.00
33		MN1	2.25	1.75
34		MN2	2.25	2.50
35		ML	2.25	2.25
36	mark12	MM1	1.25	1.50
37		MM2	1.50	1.25

Table 5.1 - continued– Composite Algorithm Measured In Relative Time

Data Element	File Number	Axis	Visually Judged Method	Derivative Method with IIR Filter
38		MN1	1.25	1.00
39		MN2	1.50	1.50
40		ML	1.00	1.25
41	mark13	MM1	0.50	0.50
43		MN1	0.50	0.50
44		MN2	1.25	1.00
45		ML	1.00	1.00
46	trial 1a	MM2	1.00	1.00
47	trial 2a	MM2	2.25	2.00
48	trial 2b	MM1	2.00	2.25
49	trial 2c	MM1	2.00	1.50
50	trial 3a	MM1	1.00	0.50
51	trial 4a	MM2	2.00	2.00
52	trial 4b	MM2	1.50	1.50
53	trial 4c	MM1	1.00	1.00
54	trial 2	MM2	0.25	0.25
55	trial 3	MM1	0.75	1.00
56	trial 3a	MN2	0.75	0.50
57	trial 4	MN2	1.00	1.00
58	trial 4a	MM1	1.00	0.75
59	trial 4b	MN2	1.00	1.00

CHAPTER VI
SUMMARY AND RECOMMENDATIONS

The previous chapters describe a system that monitors the output of a calibrated measurement device (six-component balance) and determines the 'quality' of the data in terms of raw data stability. As previously stated, this paper represents a proof of principle study. This work is not intended to be the optimal solution, but describe a process that can (when optimized) save considerable resources.

The process that determines whether a steady state condition has been achieved is implemented by an algorithm that includes both a digital filter (for the attenuation of the wide spectrum of noise present in the raw model position data) and a data processing routine to predict the steady state condition.

This chapter is a summary of the research process and the conclusions of the work contained in this thesis. The problem definition, analysis steps, and the results are summarized below:

- The Propulsion Wind Tunnel (PWT) facility is devoted to aerodynamic and propulsion integration tests at AEDC.
- Aerodynamic models tested in the PWT facility are subject to test mount vibrations and inherent oscillations, which affect the quality of force measurements.

- Current testing procedures delay acquisition for two seconds after the system null pulse has indicated the completion of a model reposition command
- Raw data sets were acquired by a stand-alone electrically isolated data acquisition machine using custom developed software. These sets were analyzed for frequency content and data quality.
- Data sets were subdivided into smaller 'areas of interest.' These smaller sets were converted to a file type that could be analyzed in MatLAB.
- This MatLAB analysis led to a filtering method and an algorithm for steady state determination.
- This developed algorithm was converted and integrated into the original acquisition software and simulation tested.

The following section details the conclusions of this research and details recommendations about future implementation of this work.

This project has shown an alternative method of determining the appropriate time to acquire data with the FAMROS data acquisition system. The current method of using a two second delay was determined by analysis of historical data. This analysis determined that after a model position adjustment, most of the transient oscillations decayed to reasonable levels after two seconds. This delay is still utilized today.

The research outlined in this paper indicates that another method exists that has the capability of reducing this delay (or increasing if necessary) in order to improve the

quality of the data acquired. This method gives a live feedback to the test conductor concerning the relative stability of the model during a test run. Later, after more evaluation and refinement, this information (presented as a Boolean value) can be added to the FAMROS data system as a conditional check for data acquisition.

The chosen filter implementation (3^{rd} order IIR) and the algorithm response time (required time system must report a true condition before operator is notified) are parameters that are adjustable depending on the test article type. The values for these parameters discussed in Chapter IV are based on experimental evidence and should be suitable for most test configurations.

RECOMMENDATIONS

Although the research result was extremely successful, several areas of this effort should be continued with future work. The primary area of development should be the architecture and configuration of the final device implementation in the Propulsion Wind Tunnel test facility.

As described in Chapter II, the data system utilized in the proof of concept study consisted of a lunchbox computer (portable PC) that runs acquisition software coded in C. This architecture is suitable for development and validation testing – but other platforms exist that should be considered for possible integration into the test facility.

The final implementation of this method could be integrated in a small custom digital signal-processing (DSP) module. This module would allow the selection of different filters and setup configurations. The output of this module should be only a Boolean value that would be sent to the test control system.

Another area of further attention would be to develop a data integration plan with the existing data system in PWT (the FAMROS system). Currently, the FAMROS system has several condition flags that must show true before data is acquired (after the two second delay). These condition flags include tunnel conditions, model attitude, and status of the model positioning system. The Boolean output of this research could be combined with these signals to control the acquisition timing.

Future improvements to the filter method are also suggested. Since the final configuration consists of an IIR lowpass filter followed with a differentiator, a single cascaded filter could reduce the processing time required for a determination. This would improve the response time of the entire system.

A final recommendation is to develop an algorithm that automatically chooses an appropriate filter based on the dynamics of the test model – which would be sent to the device prior to the test. These parameters would be based on size, weight, maximum expected forces, and other parameters.

REFERENCES

REFERENCES

[1] Rose, C.D. “A Minicomputer-Based System for the Calibration of Strain Gage Balances.” Masters Thesis, The University of Tennessee, Knoxville, TN, 1982.

[2] Roden, M.S, “Analog and Digital Communication Systems.” Upper Saddle River, NJ: Prentice-Hall, 1996

[3] Oppenheim, A. V. and R.W. Schafer. “Discrete-Time Signal Processing.” Englewood Cliffs, NJ: Prentice-Hall, 1989, pp. 311-312.

[4] Phillips, C.L. and J.M. Parr, “Signal, Systems, and Transforms.” Upper Saddle River, NJ: Prentice-Hall, 1995, pp.66 and 464.

APPENDICES

APPENDIX A.
HARDWARE LIST

Computer System
- Portable BSI Lunchbox frame PC
    - 1.2 GHz AMD Athlon Processor
    - 512MB DDR Ram
    - 16x Toshiba CD/RW

- Data Acquisition Card
    - National Instruments PCI-6052E
        - 333kHz max sampling rate
        - 16 bit A/D
        - drift: 0.0044% of full scale reading 24hr sample
    - Connecting Cable: NI - SH6868-EP
    - Breakout Box: NI - SCB-68

-Data Acquisition and Analysis Software for Realtime Implementation

    - LabWindows CVI version 6.0

APPENDIX B.
FIR FILTER COEFFICENTS

Finite Impulse Response (FIR)
Linear Phase Digital Filter Design
Remez Exchange Algorithm
Multiband Design

Filter Length = 512

Impulse Response Coefficients

h(0) =   3.68248636e-03 = h(511)
h(1) =   5.54869676e-05 = h(510)
h(2) =   5.53826399e-05 = h(509)
h(3) =   5.50435251e-05 = h(508)
h(4) =   5.42883339e-05 = h(507)
h(5) =   5.32903581e-05 = h(506)
h(6) =   5.18662804e-05 = h(505)
h(7) =   5.01906441e-05 = h(504)
h(8) =   4.80746337e-05 = h(503)
h(9) =   4.56974341e-05 = h(502)
h(10) =   4.28662461e-05 = h(501)
h(11) =   3.97831456e-05 = h(500)
h(12) =   3.62228950e-05 = h(499)
h(13) =   3.24073451e-05 = h(498)
h(14) =   2.81217219e-05 = h(497)
h(15) =   2.35532002e-05 = h(496)
h(16) =   1.85178780e-05 = h(495)
h(17) =   1.32172490e-05 = h(494)
h(18) =   7.45583717e-06 = h(493)
h(19) =   1.41666779e-06 = h(492)
h(20) = -5.09174591e-06 = h(491)
h(21) = -1.18892025e-05 = h(490)
h(22) = -1.91748643e-05 = h(489)
h(23) = -2.67762277e-05 = h(488)
h(24) = -3.48872251e-05 = h(487)
h(25) = -4.32690782e-05 = h(486)
h(26) = -5.18696077e-05 = h(485)
h(27) = -6.10873978e-05 = h(484)
h(28) = -7.06247411e-05 = h(483)
h(29) = -8.04580002e-05 = h(482)
h(30) = -9.07629244e-05 = h(481)
h(31) = -1.01329396e-04 = h(480)
h(32) = -1.12362298e-04 = h(479)
h(33) = -1.23643409e-04 = h(478)
h(34) = -1.35389136e-04 = h(477)
h(35) = -1.47367585e-04 = h(476)
h(36) = -1.59812809e-04 = h(475)
h(37) = -1.72438382e-04 = h(474)
h(38) = -1.85575134e-04 = h(473)
h(39) = -1.98845071e-04 = h(472)
h(40) = -2.12539088e-04 = h(471)
h(41) = -2.26456774e-04 = h(470)
h(42) = -2.40780638e-04 = h(469)
h(43) = -2.55265535e-04 = h(468)
h(44) = -2.70128735e-04 = h(467)
h(45) = -2.85131365e-04 = h(466)
h(46) = -3.00497785e-04 = h(465)
h(47) = -3.15975066e-04 = h(464)
h(48) = -3.31795087e-04 = h(463)
h(49) = -3.47707617e-04 = h(462)
h(50) = -3.63961317e-04 = h(461)
h(51) = -3.80265411e-04 = h(460)
h(52) = -3.96809032e-04 = h(459)
h(53) = -4.13423622e-04 = h(458)
h(54) = -4.30286100e-04 = h(457)
h(55) = -4.47122198e-04 = h(456)
h(56) = -4.64220365e-04 = h(455)
h(57) = -4.81236594e-04 = h(454)
h(58) = -4.98492504e-04 = h(453)
h(59) = -5.15612367e-04 = h(452)
h(60) = -5.32958781e-04 = h(451)
h(61) = -5.50104575e-04 = h(450)
h(62) = -5.67495417e-04 = h(449)
h(63) = -5.84458896e-04 = h(448)
h(64) = -6.02015278e-04 = h(447)
h(65) = -6.18961858e-04 = h(446)
h(66) = -6.35941568e-04 = h(445)
h(67) = -6.52773981e-04 = h(444)
h(68) = -6.69671174e-04 = h(443)
h(69) = -6.86262114e-04 = h(442)
h(70) = -7.02867529e-04 = h(441)
h(71) = -7.19070716e-04 = h(440)
h(72) = -7.35265638e-04 = h(439)
h(73) = -7.50981909e-04 = h(438)
h(74) = -7.66673708e-04 = h(437)
h(75) = -7.81821267e-04 = h(436)
h(76) = -7.96953768e-04 = h(435)
h(77) = -8.11450725e-04 = h(434)
h(78) = -8.25917967e-04 = h(433)
h(79) = -8.39644783e-04 = h(432)
h(80) = -8.53355006e-04 = h(431)
h(81) = -8.66167485e-04 = h(430)
h(82) = -8.79011649e-04 = h(429)
h(83) = -8.90750459e-04 = h(428)
h(84) = -9.02590756e-04 = h(427)
h(85) = -9.12994546e-04 = h(426)
h(86) = -9.23669944e-04 = h(425)
h(87) = -9.32186584e-04 = h(424)
h(88) = -9.41381896e-04 = h(423)
h(89) = -9.43460443e-04 = h(422)
h(90) = -9.58082008e-04 = h(421)
h(91) = -9.65313403e-04 = h(420)
h(92) = -9.69933131e-04 = h(419)
h(93) = -9.75930967e-04 = h(418)
h(94) = -9.79871905e-04 = h(417)
h(95) = -9.84008506e-04 = h(416)
h(96) = -9.86478828e-04 = h(415)
h(97) = -9.88765177e-04 = h(414)

```
h( 98) =  -9.89543229e-04 = h(413)
h( 99) =  -9.89923310e-04 = h(412)
h(100) =  -9.88850541e-04 = h(411)
h(101) =  -9.87244022e-04 = h(410)
h(102) =  -9.84212472e-04 = h(409)
h(103) =  -9.80507653e-04 = h(408)
h(104) =  -9.75418211e-04 = h(407)
h(105) =  -9.69540315e-04 = h(406)
h(106) =  -9.62244589e-04 = h(405)
h(107) =  -9.54073985e-04 = h(404)
h(108) =  -9.44487839e-04 = h(403)
h(109) =  -9.33957965e-04 = h(402)
h(110) =  -9.22002677e-04 = h(401)
h(111) =  -9.09045186e-04 = h(400)
h(112) =  -8.94658467e-04 = h(399)
h(113) =  -8.79198636e-04 = h(398)
h(114) =  -8.62250064e-04 = h(397)
h(115) =  -8.44007367e-04 = h(396)
h(116) =  -8.24505125e-04 = h(395)
h(117) =  -8.03742132e-04 = h(394)
h(118) =  -7.81410876e-04 = h(393)
h(119) =  -7.57923102e-04 = h(392)
h(120) =  -7.32833649e-04 = h(391)
h(121) =  -7.06532861e-04 = h(390)
h(122) =  -6.78617477e-04 = h(389)
h(123) =  -6.49458532e-04 = h(388)
h(124) =  -6.18664912e-04 = h(387)
h(125) =  -5.86607476e-04 = h(386)
h(126) =  -5.52865700e-04 = h(385)
h(127) =  -5.17887706e-04 = h(384)
h(128) =  -4.81187692e-04 = h(383)
h(129) =  -4.43136593e-04 = h(382)
h(130) =  -4.03508070e-04 = h(381)
h(131) =  -3.62495119e-04 = h(380)
h(132) =  -3.19825881e-04 = h(379)
h(133) =  -2.75763578e-04 = h(378)
h(134) =  -2.30050795e-04 = h(377)
h(135) =  -1.82951162e-04 = h(376)
h(136) =  -1.34200645e-04 = h(375)
h(137) =  -8.40648542e-05 = h(374)
h(138) =  -3.22894517e-05 = h(373)
h(139) =   2.08575255e-05 = h(372)
h(140) =   7.56567745e-05 = h(371)
h(141) =   1.31870661e-04 = h(370)
h(142) =   1.89682076e-04 = h(369)
h(143) =   2.48856916e-04 = h(368)
h(144) =   3.09679804e-04 = h(367)
h(145) =   3.71802158e-04 = h(366)
h(146) =   4.35574852e-04 = h(365)
h(147) =   5.00615275e-04 = h(364)
h(148) =   5.67303028e-04 = h(363)
h(149) =   6.35200910e-04 = h(362)
h(150) =   7.04762800e-04 = h(361)
h(151) =   7.75427028e-04 = h(360)
h(152) =   8.47934713e-04 = h(359)
h(153) =   9.21043128e-04 = h(358)
h(154) =   9.96139555e-04 = h(357)
h(155) =   1.07265003e-03 = h(356)
h(156) =   1.15014147e-03 = h(355)
h(157) =   1.22891799e-03 = h(354)
h(158) =   1.30894579e-03 = h(353)
h(159) =   1.39019252e-03 = h(352)
h(160) =   1.47270516e-03 = h(351)
h(161) =   1.55634477e-03 = h(350)
h(162) =   1.64121307e-03 = h(349)
h(163) =   1.72711393e-03 = h(348)
h(164) =   1.81418187e-03 = h(347)
h(165) =   1.90217383e-03 = h(346)
h(166) =   1.99129295e-03 = h(345)
h(167) =   2.08124531e-03 = h(344)
h(168) =   2.17228090e-03 = h(343)
h(169) =   2.26404714e-03 = h(342)
h(170) =   2.35687580e-03 = h(341)
h(171) =   2.45031153e-03 = h(340)
h(172) =   2.54480969e-03 = h(339)
h(173) =   2.63980138e-03 = h(338)
h(174) =   2.73589723e-03 = h(337)
h(175) =   2.83232919e-03 = h(336)
h(176) =   2.93002239e-03 = h(335)
h(177) =   3.02776160e-03 = h(334)
h(178) =   3.12747358e-03 = h(333)
h(179) =   3.22457491e-03 = h(332)
h(180) =   3.32370575e-03 = h(331)
h(181) =   3.42431850e-03 = h(330)
h(182) =   3.52404752e-03 = h(329)
h(183) =   3.62481791e-03 = h(328)
h(184) =   3.72533430e-03 = h(327)
h(185) =   3.82649659e-03 = h(326)
h(186) =   3.92748365e-03 = h(325)
h(187) =   4.02890103e-03 = h(324)
h(188) =   4.13012773e-03 = h(323)
h(189) =   4.23163143e-03 = h(322)
h(190) =   4.33288017e-03 = h(321)
h(191) =   4.43426169e-03 = h(320)
h(192) =   4.53534801e-03 = h(319)
h(193) =   4.63639195e-03 = h(318)
h(194) =   4.73708575e-03 = h(317)
h(195) =   4.83764582e-03 = h(316)
h(196) =   4.93775700e-03 = h(315)
h(197) =   5.03759431e-03 = h(314)
h(198) =   5.13688708e-03 = h(313)
h(199) =   5.23578563e-03 = h(312)
h(200) =   5.33404294e-03 = h(311)
h(201) =   5.43178377e-03 = h(310)
h(202) =   5.52880665e-03 = h(309)
h(203) =   5.62522864e-03 = h(308)
h(204) =   5.72091705e-03 = h(307)
h(205) =   5.81572049e-03 = h(306)
h(206) =   5.90963193e-03 = h(305)
h(207) =   6.00279508e-03 = h(304)
h(208) =   6.09483389e-03 = h(303)
h(209) =   6.18601589e-03 = h(302)
h(210) =   6.27600544e-03 = h(301)
h(211) =   6.36501717e-03 = h(300)
h(212) =   6.45274006e-03 = h(299)
h(213) =   6.53938498e-03 = h(298)
h(214) =   6.62463782e-03 = h(297)
h(215) =   6.70874151e-03 = h(296)
h(216) =   6.79131357e-03 = h(295)
h(217) =   6.87265673e-03 = h(294)
h(218) =   6.95248858e-03 = h(293)
h(219) =   7.03079999e-03 = h(292)
h(220) =   7.10754498e-03 = h(291)
h(221) =   7.18279671e-03 = h(290)
h(222) =   7.25636086e-03 = h(289)
h(223) =   7.32832967e-03 = h(288)
h(224) =   7.39850430e-03 = h(287)
h(225) =   7.46700603e-03 = h(286)
h(226) =   7.53362603e-03 = h(285)
h(227) =   7.59849609e-03 = h(284)
h(228) =   7.66139997e-03 = h(283)
h(229) =   7.72250725e-03 = h(282)
h(230) =   7.78159684e-03 = h(281)
h(231) =   7.83879003e-03 = h(280)
```

```
h(232) =   7.89385313e-03 = h(279)
h(233) =   7.94702235e-03 = h(278)
h(234) =   7.99794379e-03 = h(277)
h(235) =   8.04693942e-03 = h(276)
h(236) =   8.09360842e-03 = h(275)
h(237) =   8.13832796e-03 = h(274)
h(238) =   8.18061450e-03 = h(273)
h(239) =   8.22097519e-03 = h(272)
h(240) =   8.25873894e-03 = h(271)
h(241) =   8.29477683e-03 = h(270)
h(242) =   8.32760781e-03 = h(269)
h(243) =   8.35891641e-03 = h(268)
h(244) =   8.38841605e-03 = h(267)
h(245) =   8.41449705e-03 = h(266)
```

```
h(246) =   8.43862856e-03 = h(265)
h(247) =   8.46017352e-03 = h(264)
h(248) =   8.47957387e-03 = h(263)
h(249) =   8.49647607e-03 = h(262)
h(250) =   8.51111392e-03 = h(261)
h(251) =   8.52326750e-03 = h(260)
h(252) =   8.53307639e-03 = h(259)
h(253) =   8.54039487e-03 = h(258)
h(254) =   8.54530579e-03 = h(257)
h(255) =   8.54775031e-03 = h(256)
```

	Band 1	Band 2
Lower Band Edge	0.00000000	0.00650000
Upper Band Edge	0.00200000	0.49999000
Desired Value	1.00000000	0.00000000
Weighting	1.00000000	1.00000000
Deviation	0.00729839	0.00729839

APPENDIX C.
IIR FILTER COEFFICENTS

IIR Lowpass Filter Design
Elliptic Approximation
3th-Order Filter

Cascade Structure Realization:

Gain = 5.70889623e-04

* (z^2 +1.00000000 z +0.00000000) / (z^2 -0.98900879 z +0.00000000)

* (z^2 -1.99780369 z +1.00000000) / (z^2 -1.98992241 z +0.99015056)

Parallel Structure Realization:

Gain = 5.70889623e-04

+ (+0.01093081 z +0.00000000) / (z^2 -0.98900879 z +0.00000000)

+ (-0.00979981 z +0.00980093) / (z^2 -1.98992241 z +0.99015056) 0.00729839

Filter Order: 3

Filter Type: Lowpass
Band Edge Freq 1 : 0.0020
Passband Ripple (dB): $4e^{-2}$

Filter Type: Elliptic
Band Edge Freq 2: 0.0065
Stopband Attenuation (dB) 40

VITA

Martin Vincent Fette was born in Sarasota, Florida on December 5, 1971. He was raised in Gainesville, Georgia and graduated from North Hall High School in 1989. Martin entered North Georgia College and State University in Dahlonega, Georgia and received a Bachelors of Science degree in Physics in 1993. He later enrolled in the engineering program at Mercer University in Macon, Georgia and received a Bachelors of Science in Electrical Engineering in December 1996. After graduation, Martin accepted an engineering position with the Applied Technology department of Sverdrup Technology, chief testing contractor at Arnold Engineering Development Center. Once there, he continued his studies at the University of Tennessee Space Institute in Tullahoma, Tennessee. In December of 2002, Martin officially received a Master of Science degree in Electrical Engineering.